NASA CONTRACTOR REPORT

NASA CR-934

AN EXPERIMENTAL INVESTIGATION OF THE RADIAL DISPLACEMENTS OF A THIN-WALLED CYLINDER

by O. G. S. Ricardo

Prepared by
CALIFORNIA INSTITUTE OF TECHNOLOGY
Pasadena, Calif.
for

NATIONAL AERONAUTICS AND SPACE ADMINISTRATION • WASHINGTON, D. C. • NOVEMBER 1967

NASA CR-934

AN EXPERIMENTAL INVESTIGATION OF THE RADIAL DISPLACEMENTS OF A THIN-WALLED CYLINDER

By O. G. S. Ricardo

Issued by Originator as Report No. SM 67-7

Prepared under Grant No. NsG-18-59 by
CALIFORNIA INSTITUTE OF TECHNOLOGY
Pasadena, Calif.

for

NATIONAL AERONAUTICS AND SPACE ADMINISTRATION

For sale by the Clearinghouse for Federal Scientific and Technical Information
Springfield, Virginia 22151 – CFSTI price $3.00

ACKNOWLEDGMENT

The author wants to express his deep appreciation for all the help and advice he was given by Dr. E. E. Sechler, who made his work possible. He also wants to show his appreciation for the help he received in many ways from Dr. C. D. Babcock, Miss H. Burrus, Mr. M. J. Wood, and all others of the GALCIT Solid Mechanics Group.

He also wants to thank the authorities of the Escola Politecnica da Universidade de S. Paulo, of the National Aeronautics and Space Administration, of the Engineering Division of the California Institute of Technology, and of the Fulbright Committee who helped make possible his work at the GALCIT.

LIST OF SYMBOLS

A = cross-sectional area of the cylinder, sq. in.

d = imperfection depth, inches

e = eccentricity of the axial load, inches

E = Young's Modulus of Mylar, pounds per sq. in.

E_s = Young's Modulus of the seam (one overlapping Mylar strip, plus the epoxy cement) pounds per sq. in.

H = effective cylinder height, inches

I = moment of inertia of the cylinder section about the neutral axis, in.^{4}

K = ratio $\frac{P}{P_{c\ell}}$

K_{max} = $\sigma_{max}/\sigma_{c\ell}$

k = $\frac{\text{seam width}}{\text{cylinder radius}}$

P = axial load that causes collapse of the cylinder, pounds

$P_{c\ell}$ = classical buckling load = $\frac{AEt}{\sqrt{3(1-\nu^2)}\ R}$, pounds

R = radius of the middle surface of the cylinder wall, inches

t = wall thickness, inches

t_s = seam thickness, inches

w = seam width, inches

S = section modulus, = $(R + e)/I$ in.^{3}

y_g = distance from the C.G. of the cylinder (including seam) to the geometrical center, inches

σ = compressive stress, psi

$\sigma_{c\ell}$ = classical buckling load = $\dfrac{E}{\sqrt{3(1-\nu^2)}}\left(\dfrac{t}{R}\right)$ psi

σ_{b_1} = bending stress at the seam psi

σ_{b_2} = bending stress opposite to the seam psi

ν = Poisson's ratio

AN EXPERIMENTAL INVESTIGATION OF THE RADIAL DISPLACEMENTS OF A THIN WALLED CYLINDER

By O. G. S. Ricardo*

ABSTRACT

A series of experiments have been carried out in order to determine the behavior of the wall of a circular cylinder loaded in axial compression. One case considered was when the wall was subjected to an initial displacement by a point radial load. A second case measured wall displacements with no side loads or initial displacements and the third case considered the change in an initial permanent deformation in the thin wall of the cylinder. The data obtained indicate the behavior of such cylinders near the collapse load.

INTRODUCTION

The improvement of experimental techniques of manufacturing thin-walled cylindrical shells and of controlling their boundary conditions has made it possible to more accurately match the theoretical buckling loads with those obtained experimentally, (Ref. 1, 2, 3). However the mechanism leading to collapse is still not fully understood. The purpose of this investigation was to get information concerning the behavior of the cylinder wall under various conditions in the hope that this information would eventually contribute to the clarification of the buckling process. In order to accomplish this, the following series of

---

* Research Associate at the California Institute of Technology during preparation of this report.

experiments were carried out in thin-walled circular cylinders made of Mylar. These cylinders had an R/t ratio of approximately 400.

1. An imperfection was impressed in the cylinder wall by a point radial load and the cylinder was then subjected to an increasing axial load. The effect of changes in the depth of this imperfection on the axial load was recorded. A further variable was the eccentricity of the axial load to the cylinder.

2. A cylinder with no initial imperfections was tested with increasing axial load while radial displacements of several points on the cylinder wall were measured. Displacement measurements were taken from zero axial load up to the final collapse load.

3. One permanent imperfection was imposed on the cylinder wall and the action of the wall in the vicinity of this imperfection was studied as the axial load was increased to buckling. The displacements of points on the cylinder generator passing through the permanent imperfection were measured as a function of the axial load.

Experimental Set-Up

The general experimental system is shown in Fig. 1. The cylinder had a 4 inch radius and was made of 0.010 inch thick Mylar sheet. Mylar was used because of its recovery properties that permit it to be rebuckled many times without lowering the buckling stress of the specimen. The specimen was 11 inches long with an extra 1/2 inch at each end which was cast into grooves in aluminum plates with Cerrolow 117 low melting point alloy. In order to obtain good end fixity and uniform loading, 1/8 inch holes were punched in the end areas so that the Cerrolow could flow through and give a good lock to the edges. The seam in all cases was 1/2 inch wide and the bonding agent was epoxy cement.

Load was applied by a standard testing machine but was measured by the load recording system shown. This consisted of four small Mylar cylinders about 1 1/4 inches high and 1 inch in diameter. Strain gages were cemented to these cylinders and their output was fed into a strain gage bridge. Mylar was used because the loads expected were very low and the low modulus of Mylar gave reasonable gage outputs for these low loads. The load measuring system was calibrated and found to be sufficiently linear over the ranges desired.

Displacement measurements were made with a reluctance type pick-up which did not require mechanical contact with the cylinder wall. Because such a pick-up only measures deflections of metal surfaces, small (7/16" diameter) circles of aluminum foil (0.002" thick) were cemented to the Mylar surface with a small (0.005" diameter) spot of epoxy cement. The deflection read was considered to be the deflection

of the center point of this aluminum circle and rotation effects were neglected. The pick-up was initially centered in front of the metallic circle at a distance of from 0.06 to 0.10 inches. With this system it was possible to read radial deflections as small as 10^{-4} inches.

In the first and second series of experiments, calibration readings were made for every point. As the pick-up was inside the specimen, a pointer on a calibrated screw (reading to 10^{-3}) inches) could be pushed against the cylinder wall from the outside thus getting a direct measurement calibration. For the third series of experiments the pick-up was placed outside the cylinder and no calibration was made. However, from the calibration results of the other two cases, the calibration could be estimated and, as will be shown later, the results are consistent.

In the first series of experiments, the collapse load in the cylinder was measured as a function of wall displacements. In the second and third series, a plotter was used which gave the displacement of a point in the cylinder as a function of the load. Both sets of instrumentation had relatively large time constants which did not affect the recording of the loading branch of the curves. For points beyond buckling (post-buckling) only the initial buckling point can be considered as valid.

First Series of Experiments

In previous studies by the author (Ref. 4), dimples with increasing depths were imposed on Mylar and brass cylinders and the axial load was increased from zero to the collapse load while the

changes in depth of these dimples was observed. The dimples were produced by a lever system with dead weight loading giving a constant radial point force in the cylinder wall. Three distinct regions could be observed:

a. For dimple depths up to about 1.5 t there was no influence on the buckling load.

b. For $1.5 \leq \frac{d}{t} \leq 2.0$ there was a sharp drop in the collapse load.

c. For $\frac{d}{t} > 2.0$ the collapse load decreased slowly with an increase in $\frac{d}{t}$ and a local large wave appeared before collapse.

For these specimens collapse occurred for an axial load of the order of 45 $^{o}/o$ of the theoretical load. Since the constancy of the collapse load for the displacements of the order of the wall thickness could be of importance, it was decided to repeat the experiment with the new testing equipment.

Series I - Test Results

In order to take into account the dissymmetry caused by the seam, one cylinder was loaded at loading points on the diameter containing the seam and at various distances from the geometric center. For notations see Fig. 2 and for the cylinder properties as affected by the seam see Appendix I. The results of this set of tests are shown in Table I and plotted in Fig. 3.

The initial cylinder imperfections were relatively low as indicated by the fact that the maximum buckling stress was nearly 70 °/o of the classical value which is what would be expected from previous test on cylinders with ends restrained against radial motion. The curve of P vs. eccentricity is symmetric about an eccentricity of 3/16 inch indicating that this is the location of the stiffness center of the cylinder. This value of 3/16 = 0. 187 inch must be compared with the predicted value of 0. 078 inch from Appendix I. Although the agreement is not exact, the value of y_g is of the correct sign and the right order of magnitude. Differences between the measured and calculated values may occur for several reasons, including possible cylinder imperfections, effects of clamping the seam at the ends, or non-uniform values of seam thickness which would affect the effective seam modulus. It will also be noted from the location of the buckling band in Fig. 3 that the true stiffness center is probably not exactly on the diameter passing through the seam. This fact has been ignored in the study.

The second phase of this series of test was concerned with the effect of an imposed imperfection. The imposed imperfection, of depth d, was always located in the center of the cylinder height and directly opposite the seam. Table II and Fig. 4 gives the results of this set of tests. The conclusion from this set of experiments can be summarized as follows:

1. The maximum buckling stress (axial compression plus bending) lies in the range of 0. 65 - 0. 71 times the classical buckling stress.

2. An imposed dimple does not change the maximum buckling stress until the dimple depth has reached a magnitude of 1.5 - 2.0 times the cylinder sheet thickness after which it falls to approximately half of the classical value remaining at this level for deformations up to at least 7 times the sheet thickness.

3. In some cases (eccentricity in the direction of the deformation) an initial wave pattern was formed at a somewhat lower stress value ($\sigma/\sigma_{c\ell} \sim 0.45$) but complete collapse did not occur until a value of $\sigma/\sigma_{c\ell} = 0.50$ was reached.

4. Moving the eccentricity away from the initial deformation tended to delay the point where the initial deformation took effect and to increase the final collapse value a small account. In this case, below the critical value of d/t, collapse takes place on the side opposite the deformation where the maximum stress is highest. Above d/t critical, the deformation induces the collapse and the buckling band is in the side of the initial deformation.

The critical value of d/t as a function of the load distance from the neutral axis is shown in Fig. 5. Plus values of eccentricity give tension bending stresses at the deformation.

A typical shape of the imposed deformation is shown in Fig. 6. Curvatures in the circumferential direction are seen to be much larger than those in the axial direction.

Second Series of Experiments

The second series of experiments was designed to determine the shape of the cylinder just before buckling and to determine the radial deformation at specific points as a function of the applied axial load. As only one displacement pick-up was available, it was necessary to rely on the fact that a Mylar cylinder would give repeatable results for many loadings. In order to definitely locate the buckle area of the cylinder a relatively large eccentricity was used to force the buckling to take place in a specific place around the specimen. Thus, the real eccentricity used was 5/16" opposite to the seam, and displacements were measured over a sector angle of 120^{o} opposite to the seam and, in the axial direction, somewhat more than half the height of the cylinder from one end was covered. At least three displacement - load curves were measured for each point. As the cylinder had to be removed from the testing machine to relocate the pick-up to a new point, slight variations due to alignment changes probably occurred. Also, the displacement readings were so small as to require the equipment to be working at its maximum sensitivity and thus down near the "noise" level. For this reason, the results should be evaluated more on qualitative than a quantitative basis although the order of magnitude of the radial displacements is correct.

Series II - Test Results

Typical displacement vs. load curves for three points are shown in Figs. 7a, b, and c. These show the repeatability of the curves for multiple loading and it was this repeatability that gave

confidence in the method. Cross-faired circumferential and axial plots of the radial formation just prior to buckling are shown in Figs. 8 and 9 and a surface plot is shown in Fig. 10. These curves show the following results:

1. That a definite wave pattern has been established just before buckling with a maximum amplitude of about 1/3 the sheet thickness.
2. That the curvatures in the axial direction are generally much lower than those in the circumferential direction.
3. That the circumferential wave pattern has a wave length corresponding to approximately 45^{o} of circumferential angle. This wave length is very nearly equal to the wave length of the diamond-shaped buckles which form at collapse.
4. Appreciable non-linearity is shown in only two regions (see Fig. 10) and it is probably these two regions which precipitate collapse.

Since the recording apparatus was too slow to follow the post-buckling deformation, the load-deformation waves beyond the collapse point in Fig. 7 are not to be considered accurate. Curves with considerable non-linearity as in Figs. 7b and 7c show that displacements are increasing rapidly where they reach 20 - 40 $^{o}/o$ of the sheet thickness corresponding in magnitude to the values of d/t critical of 1.5 to 2 found in Series I.

Third Series of Experiments

These tests were made to watch the development of a local imperfection into a large diamond shaped wave. The set-up is shown in Fig. 11 and the permanent initial deformation (made by locally loading the shell surface until yielding took place) was located at point 2 (11/16" from the end of the cylinder). This region was chosen because it was believed, at the time, that initial deformations near the fixed end of the cylinder would have the most serious effect in the buckling stress. Measurements were taken by attaching 7/16" diameter aluminum foil discs along the generator through the initial deformation and reading the change in displacement by the usual reluctance pick-up. Again, repeatability of the Mylar was assumed and checked by duplicate runs in the same point.

Series III - Test Results

The repeatability of the load-deformation curves for separate loading is shown in Fig. 12 and 13. The displacement along the generator is shown in Fig. 14 for various load conditions. From these figures the following observations can be made:

1. A small region of local instability develops around the initial deformation at point 2.
2. That collapse occurs when the displacement at point 2 has built up to approximately twice the thickness. This agrees again with the first series of tests.
3. At points 3 to 8 there are displacement sense reversals just before collapse.

4. After collapse, and the formation of diamond waves, the center of the first wave is at point 4 showing a sudden jump to the stable post-buckling wave form.

The first formation of the diamond wave occurred at 0.45 $P_{c\ell}$ and final collapse occurred at 0.47 $P_{c\ell}$. This also agrees with the general results of the first series of tests.

Fig. 15 shows some of the complex displacements that can take place in a cylinder as the load increases. Considering point No. 22 which is very close (1/4") to the fixed edge we see that first it has an outward radial deformation which is nearly linear and which corresponds to the Poisson expansion. Then, due possibly to some development of a circumferential wave pattern, the deformation goes from positive to negative. Finally, just before collapse the sign again reverses and large positive deformation occurs as collapse takes place.

Conclusions and Recommendations

1. For cylinders under axial load and a given boundary condition there will be a buckling load which is a certain percentage of the classical buckling load. For the present set of tests this percentage is from 65 $^{o}/o$ to 75 $^{o}/o$. Other tests at GALCIT indicate that this amount of reduction from the classical value is probably due to the restraint against outward expansion at the ends of the cylinder (prevention of Poisson expansion) which causes an initial deformation at the ends.

2. That, for dimple-type initial deformations, no reduction in the above collapse load occurs until the ratio of the dimple depth to the hickness reaches a value of 1.5 to 2.0. The actual value of this initial d/t value depends upon the type of loading (e.g. - ratio of bending to axial stress).

3. That there is a small but finite wave pattern established in the cylinder just before collapse takes place and, at least for these experiments, the circumferential wave length of this wave pattern is essentially equal to the diamond shape post-buckling pattern.

4. With sufficiently large initial deformation ($d/t > d/t_{cr}$) there appears to be a lower bound for the collapse load which is of the order of $0.5\ P_{c\ell}$ - at least for values of d/t up to 7.0.

Further research problems that are indicated by the above results are:

1. Determine if d/t_{cr} approaches zero for an essentially perfect cylinder. This would mean that $P \longrightarrow P_{c\ell}$. Such a phenomenon is indicated by some of the recent work of the GALCIT group for plated cylinders which are essentially perfect.

2. Attempt to correlate the displacements before collapse with initial deformations. To do this correctly, an overall picture of the initial state of the cylinder is needed as well as a means of following the initial displacements during loading. Such a system has been designed and is now being checked out.

3. Investigate the effect of location as well as size of an initial deformation in the buckling load and determine how each form of initial deformation changes as the load increases up to collapse.

APPENDIX I

GEOMETRICAL PROPERTIES OF CYLINDER WITH SEAM

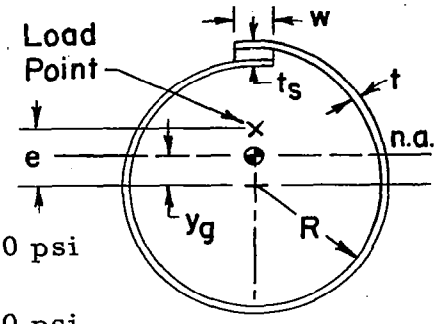

w = width of seam = 0.5 in.

t_s = thickness of seam = 0.025 in.

E_s = Young's modulus of seam = 600,000 psi

E = Young's modulus of Mylar = 725,000 psi

t = cylinder wall thickness = 0.010 in.

R = cylinder radius = 4 in.

ν = Poisson's ratio = 0.3

The effective area is given by

$$A = 2\pi RT + w\left[t_s \frac{E_s}{E} - t\right] = 0.256 \text{ sq. in.}$$

Location of neutral axis is given by

$$y_g = w\left[t_s \frac{E_s}{E} - t\right] R/A = 0.078 \text{ in.}$$

Moment of inertia is

$$I = \pi R^3 t + 2\pi R t y_g^2 + w(R - y_g)^2 \left(t_s \frac{E_s}{E} - t\right) = 2.09 \text{ in.}^4$$

$$\sigma_{b_1} = \frac{\left(P_{e_{exp}}\right)\left[R - y_g(exp)\right]}{I}$$

$$\sigma_{b_2} = \frac{\left(P_{e_{exp}}\right)\left[R + y_g(exp)\right]}{I}$$

APPENDIX II

CLASSICAL LOAD FOR THE SPECIMEN

$$\sigma_{c\ell} = E \frac{t}{R} \frac{1}{\sqrt{3(1 - \nu^2}}$$

Using Poisson's Ratio $\nu \cong 0.3$ for Mylar

$$\sigma_{c\ell} = 725,000 \cdot \frac{0.010}{4} \cdot \frac{1}{1.65} = 1,090 \text{ psi}$$

$$P_{c\ell} = A \cdot \sigma_{c\ell} = 0.256 \cdot 1090 = 280 \text{ pounds}$$

Radius expansion due to Poisson's Ratio, for $K = 0.66$ (Ref. Table I)

Assuming $\nu = 0.3$

$$\Delta R = \nu \varepsilon R = 0.3 \frac{\sigma}{E} R = 0.3 \frac{733}{725,000} 4 = 0.00122 \text{ in.}$$

REFERENCES

1. Babcock, C. D., and Sechler, E. E.: The Effect of Initial Imperfections in the Buckling Stress of Cylindrical Shells. Collected papers in Instability of Shell Structures. NASA TN D-1510, 1962.
2. Babcock, C. D., and Sechler, E. E.: The Effect of End Slope on the Buckling Stress of Cylindrical Shells. NASA TN D-2537, December 1964.
3. Sechler, E. E.: (Principal Investigator), Status Report No. 9 - On the Buckling of Cylindrical Shells. Graduate Aeronautical Laboratories, California Institute of Technology, Pasadena, California, NASA Grant No. NsG-18-59, July 1965.
4. Ricardo, O. G. S.: An Experimental Study on the General Buckling of Thin-Walled Circular Cylinders under Axial Loads. Internal Report. Guggenheim Aeronautical Laboratory, California Institute of Technology, 1960.
5. Ricardo, O. G. S.: Experiments on the Buckling of Cylinders. Doctorate Thesis, Polytechnic School of the University of S. Paulo, Brazil, 1964.

TABLE I

BUCKLING LOAD VS ECCENTRICITY

e	P	k	σ_c	e_{exp} **	σ_{b_1}	σ_{b_2}	σ_{TOT_1}	σ_{TOT_2}	K_{max}
in.	lb	$=P/P_{c\ell}$ *	psi.	in.	psi.	psi.	psi.	psi.	$=\sigma_m/\sigma_{c\ell}$
-1/8	167.7	0.599	-655	-5/16	+97	-107	-558	-762	0.697
0	174.0	0.621	-680	-3/16	+59	-65	-621	-745	0.682
1/16	180.0	0.643	-703	-1/8	+41	-45	-562	-748	0.684
1/8	183.6	0.656	-717	-1/16	+21	-23	-698	-742	0.679
3/16	184.4	0.659	-720	0	0	0	-720	-720	0.659
1/4	184.0	0.657	-719	1/16	-21	+23	-740	-696	0.677
5/16	180.4	0.644	-705	1/8	-41	+45	-746	-660	0.683
3/8	174.2	0.622	-680	3/16	-59	+65	-739	-615	0.676
1/2	167.7	0.599	-655	5/16	-97	+107	-752	-548	0.688

y_g (exp) = 3/16" = 0.1875"

* $P_{c\ell}$ = 280 lb.

** From Fig. 3

$\sigma_{c\ell} = P_{c\ell}/A = -1093$ psi.

TABLE IIa

EFFECT OF INITIAL DEFORMATION

Load Eccentricity = 1/8" Opposite Seam = -0.125"

Distance of Load from Neutral Axis = 5/16 = 0.3125"

σ_{b_1} = 0.3125 P x 3.8125/2.09 = 0.570 P

σ_{b_2} = 0.3125 P x 4.1875/2.09 = -0.626 P

d/t	P	σ_c	σ_{b_1}	σ_{b_2}	σ_{TOT_1}	σ_{TOT_2}	K_{max}
	lb	psi.	psi.	psi.	psi.	psi.	
0	171	-668	97	-107	-571	-775	0.711
0.14	170	-664	97	-106	-567	-770	0.706
0.23	169	-660	96	-106	-564	-766	0.703
0.32	167	-652	95	-105	-557	-757	0.694
0.46	168	-656	96	-105	-560	-761	0.698
0.58	168	-656	96	-105	-560	-761	0.698
0.68	168	-656	96	-105	-560	-761	0.698
0.90	171	-668	97	-107	-571	-775	0.711
1.01	170	-664	97	-106	-567	-770	0.706
1.10	170	-664	97	-106	-567	-770	0.706
1.30	170	-664	97	-106	-567	-770	0.706
1.47	168	-656	96	-105	-560	-761	0.698
1.49	169	-660	96	-106	-564	-766	0.703
1.57	165	-644	94	-103	-550	-746	0.684
1.60	163	-637	93	-102	-544	-739	0.678
1.60	161	-629	92	-101	-537	-730	0.670
1.67	160	-625	91	-100	-534	-725	0.665

TABLE IIa (cont'd.)

EFFECT OF INITIAL DEFORMATION

Load Eccentricity = 1/8" Opposite Seam = -0.125"

Distance of Load from Neutral Axis = 5/16 = 0.3125"

σ_{b_1} = 0.3125 P x 3.8125/2.09 = 0.570 P

σ_{b_2} = 0.3125 P x 4.8175/2.09 = 0.626 P

d/t	P	σ_c	σ_{b_1}	σ_{b_2}	σ_{TOT_1}	σ_{TOT_2}	K_{max}
	lb	psi.	psi.	psi.	psi.	psi.	
1.78	156	-609	89	-98	-520	-707	0.649
1.87	152	-594	87	-95	-507	-689	0.632
1.99	150	-586	86	-94	-500	-680	0.624
2.07	145	-566	83	-91	-483	-657	0.603
2.17	142	-555	81	-89	-474	-644	0.591
One Initial Wave							
3.15	116	-453	66	-73	-387	-526	0.482
3.16	118	-461	67	-74	-394	-535	0.491
5.00	111	-434	63	-69	-371	-503	0.461
Collapse							
3.70	122	-477	70	-76	-407	-553	0.507
3.80	125	-488	71	-78	-417	-566	0.519
5.40	126	-492	72	-79	-420	-571	0.524

TABLE IIb

Load Eccentricity = 3/16" Towards Seam = +0.1875

Distance of Load from Neutral Axis = 0 (Therefore, no bending)

d/t	P lb	σ_c psi.	K_{max}
0	187	732	0.672
0.20	190	741	0.680
0.22	184	720	0.661
0.25	183	716	0.657
0.36	185	723	0.663
0.60	185	723	0.663
0.69	183	716	0.657
1.10	186	728	0.668
1.48	185	723	0.663
1.55	184	720	0.661
1.60	185	723	0.663
1.70	183	716	0.657
1.70	179	701	0.643
1.75	177	693	0.636
1.80	177	693	0.636
1.88	174	681	0.625
2.30	162	632	0.580
5.00	140	548	0.503

TABLE IIc

Load Eccentricity = 1/4" Towards Seam = +0.250"

Distance of Load from Neutral Axis = -0.0625"

σ_{b_1} = -0.0625 P x 3.8125/2.09 = -0.1140 P

σ_{b_2} = 0.0625 P x 4.1875/2.09 = 0.1252 P

d/t	P	σ_c	σ_{b_1}	σ_{b_2}	σ_{TOT_1}	σ_{TOT_2}	K_{max}
	lb	psi.	psi.	psi.	psi.	psi.	
0	188	-734	-21	24	-755	-710	0.693
0.21	185	-723	-21	23	-744	-700	0.683
0.27	184	-719	-21	23	-740	-696	0.679
0.35	182	-711	-21	23	-732	-688	0.672
0.53	185	-723	-21	23	-744	-700	0.683
0.62	185	-723	-21	23	-744	-700	0.683
0.78	184	-719	-21	23	-740	-696	0.679
1.20	183	-715	-21	23	-736	-692	0.675
1.51	184	-719	-21	23	-740	-696	0.679
1.68	185	-723	-21	23	-744	-700	0.683
1.70	185*	-723	-21	23	-744	-700	0.683
1.70	187	-730	-21	23	-751	-707	0.689
1.90	184*	-719	-21	23	-740	-696	0.679
1.92	184*	-719	-21	23	-740	-696	0.679
1.96	180*	-703	-20	22	-723	-681	0.663
2.22	165*	-645	-19	21	-664	-624	0.609
2.30	169*	-660	-19	21	-679	-639	0.623
2.70	149*	-582	-17	19	-599	-563	0.550
3.20	141*	-551	-16	18	-567	-553	0.520

One Initial Wave

TABLE IIc (cont'd.)

Load Eccentricity = 1/4" Towards Seam = +0. 250"

Distance of Load from Neutral Axis = -0. 0625"

σ_{b_1} = 0. 625 P x 3. 8125/2. 09 = -0. 1140 P

σ_{b_2} = 0. 625 P x 4. 1875/2. 09 = 0. 1252 P

d/t	P	σ_c	σ_{b_1}	σ_{b_2}	σ_{TOT_1}	σ_{TOT_2}	K_{max}
	lb	psi.	psi.	psi.	psi.	psi.	
3. 20	138*	-539	-16	17	-555	-522	0. 509
5. 10	114*	-445	-13	14	-458	-431	0. 420
Collapse							
3. 32	141*	-551	-16	18	-567	-533	0. 520
5. 10	144*	-563	-16	18	-579	-545	0. 531
5. 40	142*	-555	-16	18	-571	-537	0. 524

* Buckle Band On Side of Dimple (Opposite Seam) Otherwise, Buckle Band On Seam Side (Opposite Deformation).

TABLE IId

Load Eccentricity = 3/8" Towards Seam = +0.375"

Distance of Load from Neutral Axis = -3/16" = -0.1875

σ_{b_1} = -0.1875 P x 3.8125/2.09 = -03420 P

σ_{b_2} = 0.1875 P x 4.1875/2.09 = 0.3757 P

d/t	P	σ_c	σ_{b_1}	σ_{b_2}	σ_{TOT_1}	σ_{TOT_2}	K_{max}
	lb	psi.	psi.	psi.	psi.	psi.	psi.
0	178	-695	-61	67	-756	-628	0.694
0.29	179	-699	-61	67	-760	-632	0.697
0.35	178	-695	-61	67	-756	-628	0.694
0.45	179	-699	-61	67	-760	-632	0.697
0.56	179	-699	-61	67	-760	-632	0.697
0.67	182	-711	-62	68	-773	-643	0.709
0.72	177	-691	-61	66	-752	-625	0.690
0.86	179	-699	-61	67	-760	-632	0.697
1.27	178	-695	-61	67	-756	-628	0.694
1.51	177	-691	-61	66	-752	-625	0.690
1.67	176	-688	-60	66	-748	-622	0.686
1.77	179	-699	-61	67	-760	-632	0.697
1.99	179	-699	-61	67	-760	-632	0.697
2.02	176	-688	-60	66	-748	-622	0.686
2.05	177*	-691	-61	66	-752	-625	0.690
2.08	181	-707	-62	68	-769	-639	0.706
2.17	184	-719	-63	69	-782	-650	0.717
2.24	171*	-668	-58	64	-726	-604	0.666
2.36	174*	-680	-60	65	-740	-615	0.679
2.38	176*	-688	-60	66	-748	-622	0.686

TABLE IId (cont'd.)

Load Eccentricity = 3/8" Towards Seam = +0.375"

Distance of Load from Neutral Axis = -3/16" = -0.1875

σ_{b_1} = -0.1875 P x 3.8125/2.09 = -0.3420 P

σ_{b_2} = 0.1875 P x 4.1875/2.09 = 0.3757 P

d/t	P	σ_c	σ_{b_1}	σ_{b_2}	σ_{TOT_1}	σ_{TOT_2}	K_{max}
	lb	psi.	psi.	psi.	psi.	psi.	psi.
2.66	158*	-617	-54	59	-671	-558	0.616
3.27	149*	-582	-51	56	-633	-526	0.581
5.00	151*	-590	-52	57	-642	-533	0.589
7.00	145*	-566	-50	54	-616	-512	0.565
7.00	149*	-582	-51	56	-633	-526	0.581

* Buckle Band On Side Of Dimple (Opposite Seam) Otherwise, Buckle Band On Seam Side (Opposite Deformation).

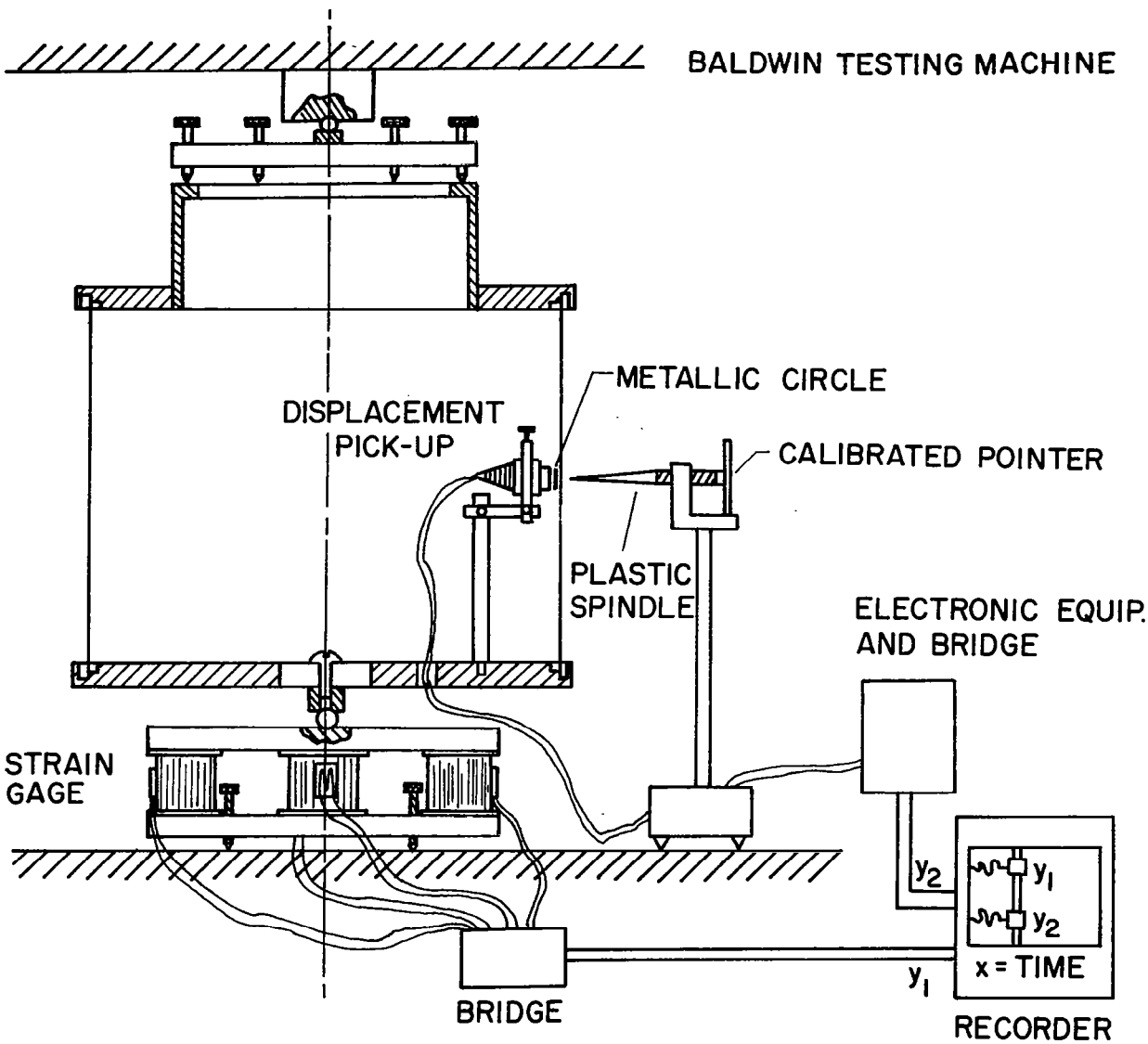

FIG. 1a EXPERIMENTAL ASSEMBLY

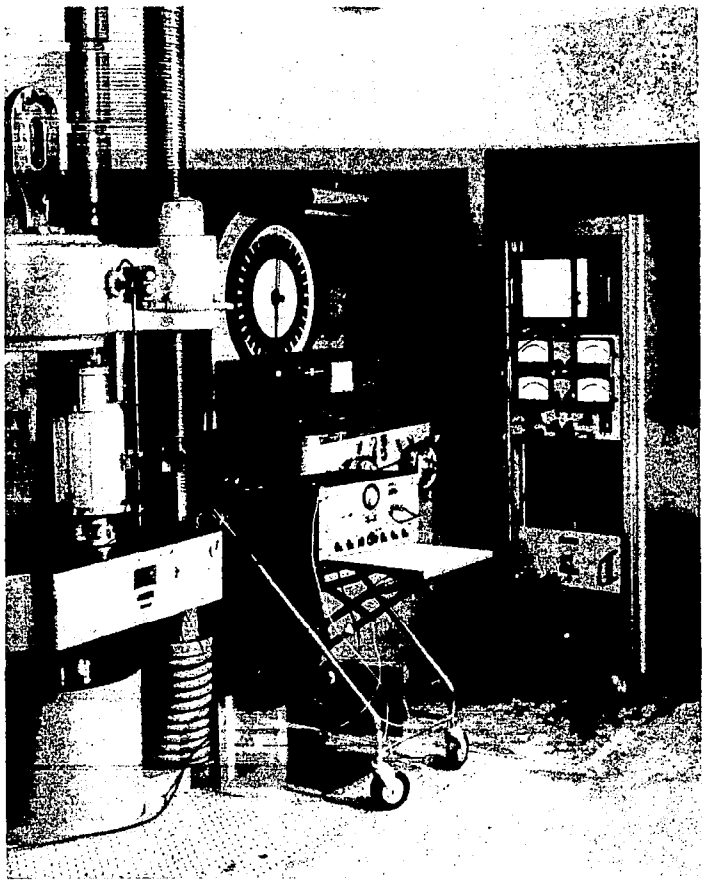

FIG. 1 b

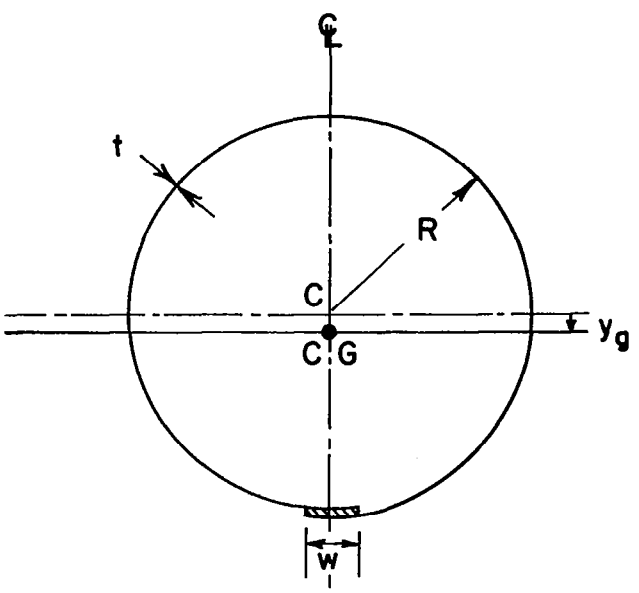

C = GEOMETRICAL CENTER
CG = CENTER OF GRAVITY
w = SEAM WIDTH

FIG. 2 CYLINDER NOTATION

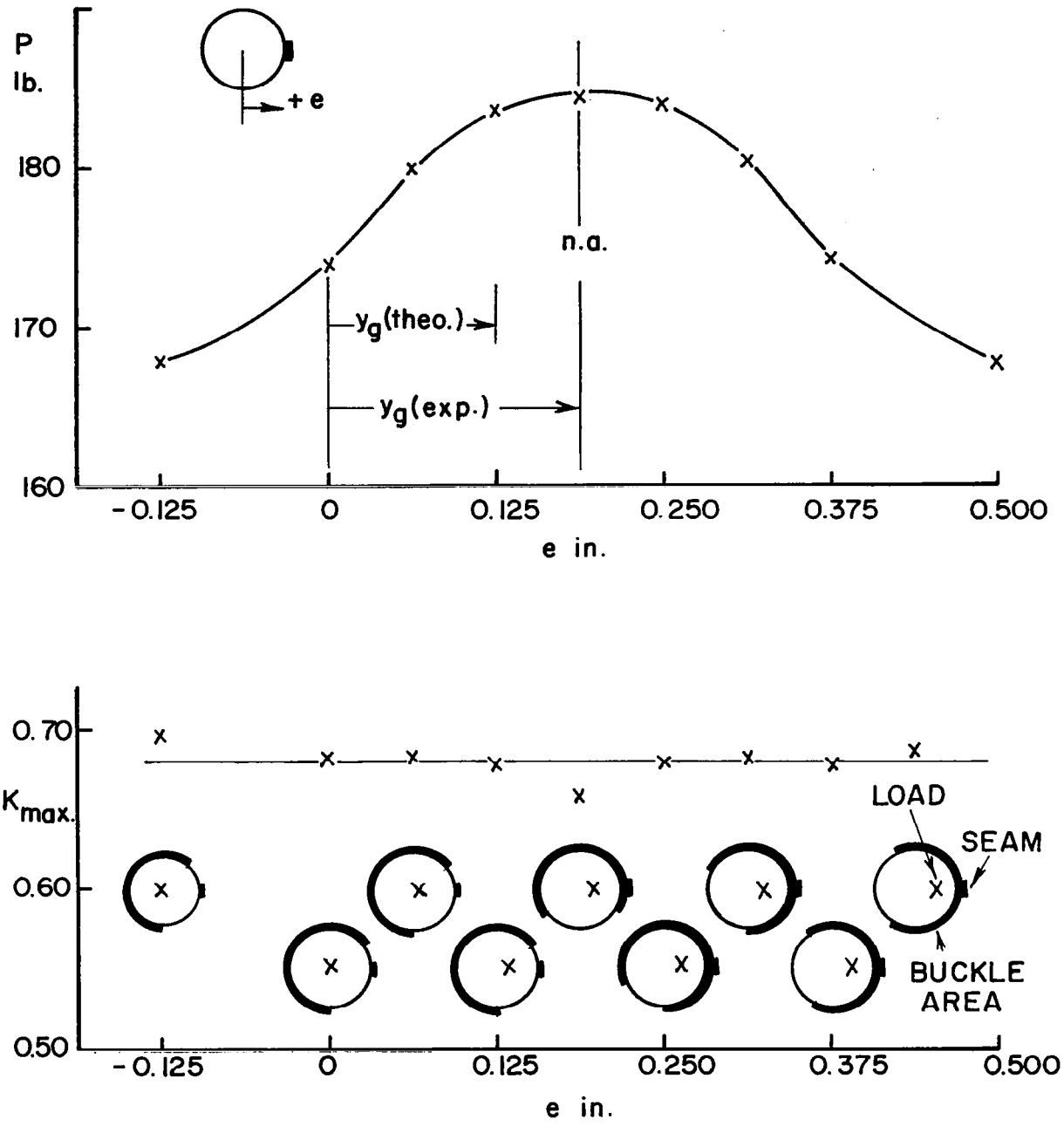

FIG. 3 BUCKLING LOAD VS. ECCENTRICITY

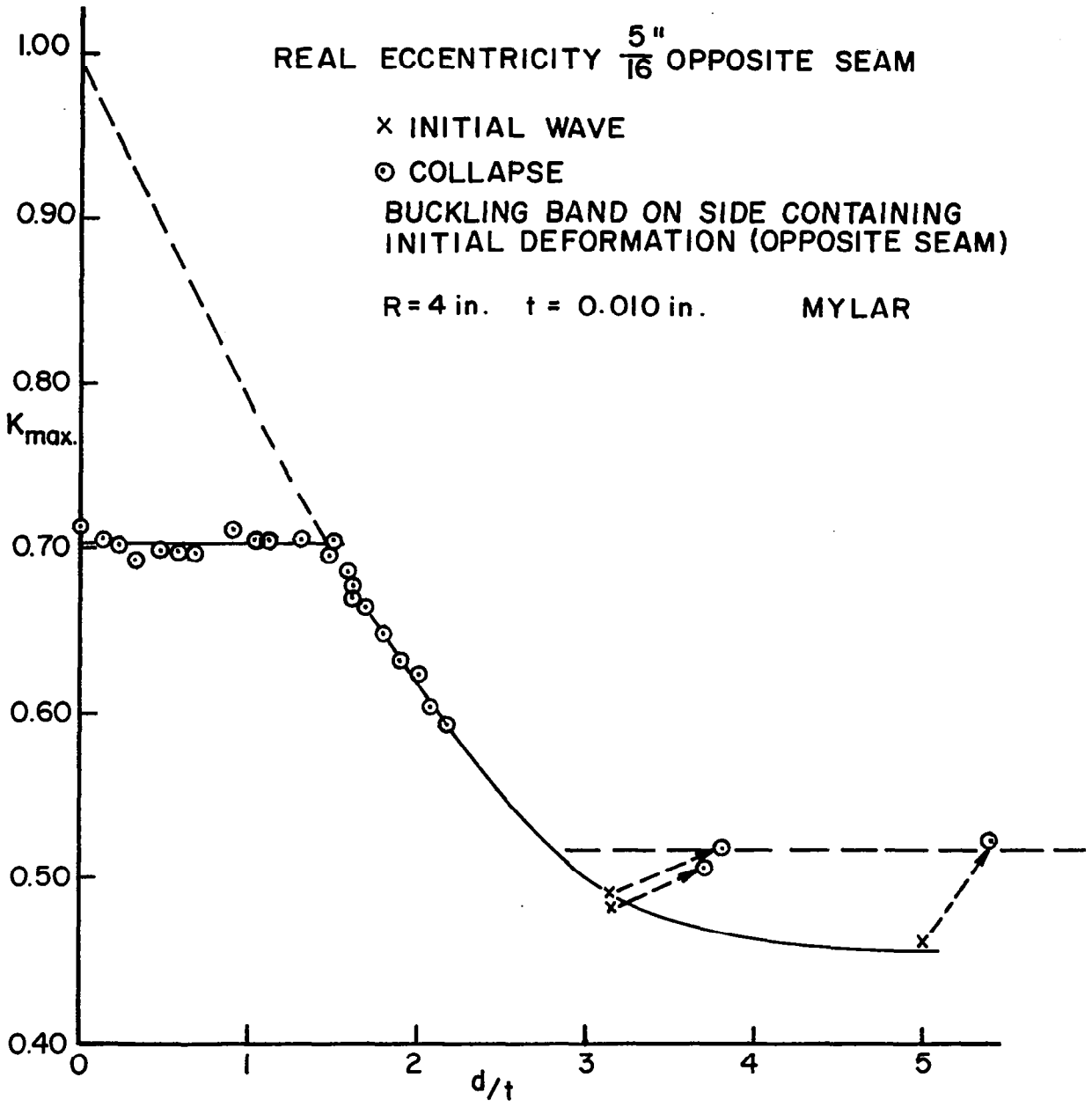

(a)

FIG. 4 EFFECT OF INITIAL DIMPLE OF DEPTH d

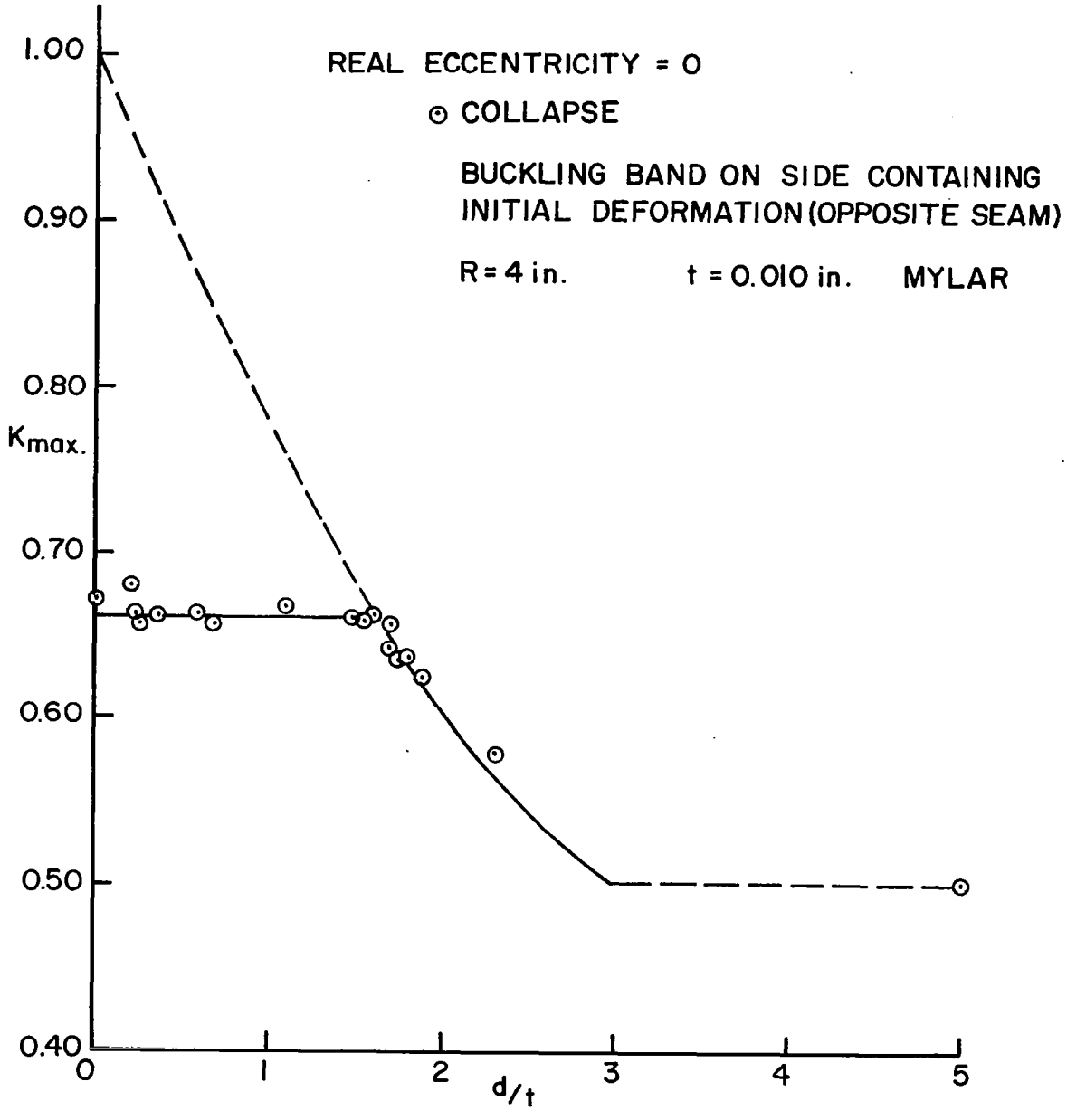
REAL ECCENTRICITY = 0
⊙ COLLAPSE
BUCKLING BAND ON SIDE CONTAINING INITIAL DEFORMATION (OPPOSITE SEAM)
R = 4 in.
t = 0.010 in.
MYLAR
1.00
0.90
0.80
Kmax.
0.70
0.60
0.50
0.40
0
1
2
3
4
5
d/t

(b)

FIG. 4 (Con't.)

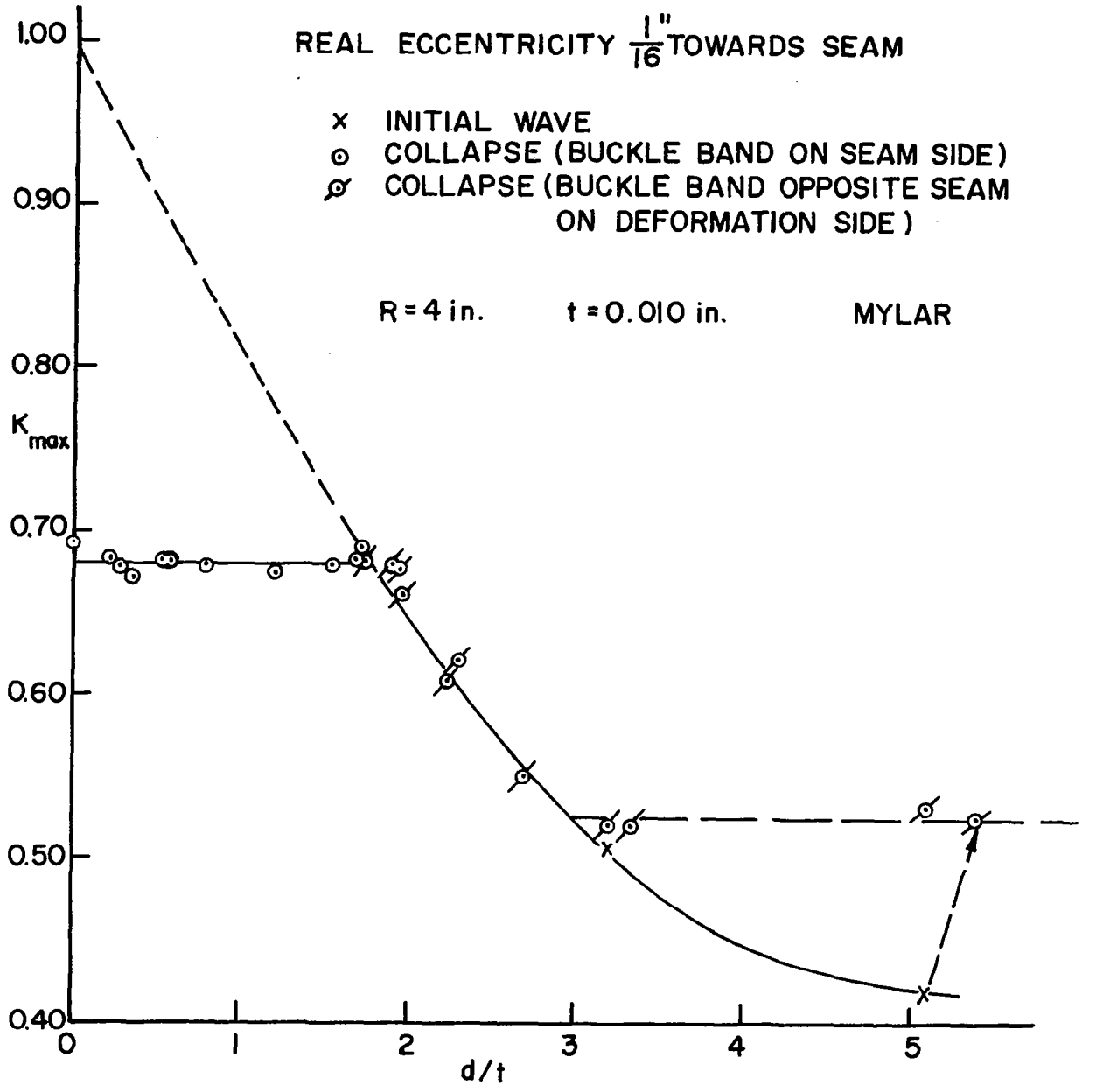
REAL ECCENTRICITY 1/16" TOWARDS SEAM
× INITIAL WAVE
⊙ COLLAPSE (BUCKLE BAND ON SEAM SIDE)
⊙ COLLAPSE (BUCKLE BAND OPPOSITE SEAM ON DEFORMATION SIDE)
R = 4 in.
t = 0.010 in.
MYLAR
1.00
0.90
0.80
K max
0.70
0.60
0.50
0.40
0
1
2
3
4
5
d/t

(c)

FIG. 4 (Con't.)

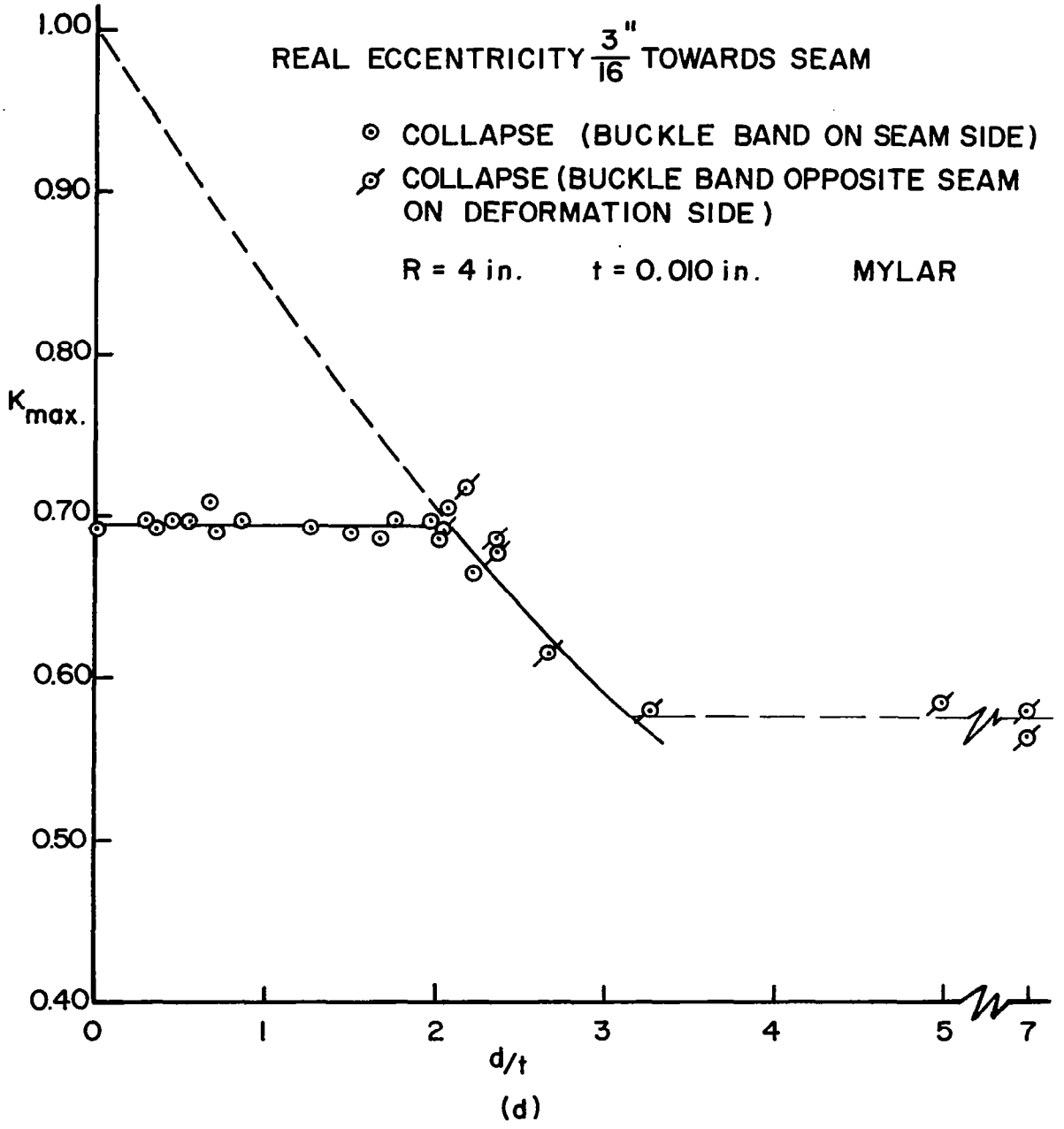
REAL ECCENTRICITY 3/16" TOWARDS SEAM
COLLAPSE (BUCKLE BAND ON SEAM SIDE)
COLLAPSE (BUCKLE BAND OPPOSITE SEAM ON DEFORMATION SIDE)
R = 4 in.
t = 0.010 in.
MYLAR
1.00
0.90
0.80
K max.
0.70
0.60
0.50
0.40
0
1
2
3
4
5
7
d/t
(d)

FIG. 4 (Con't.)

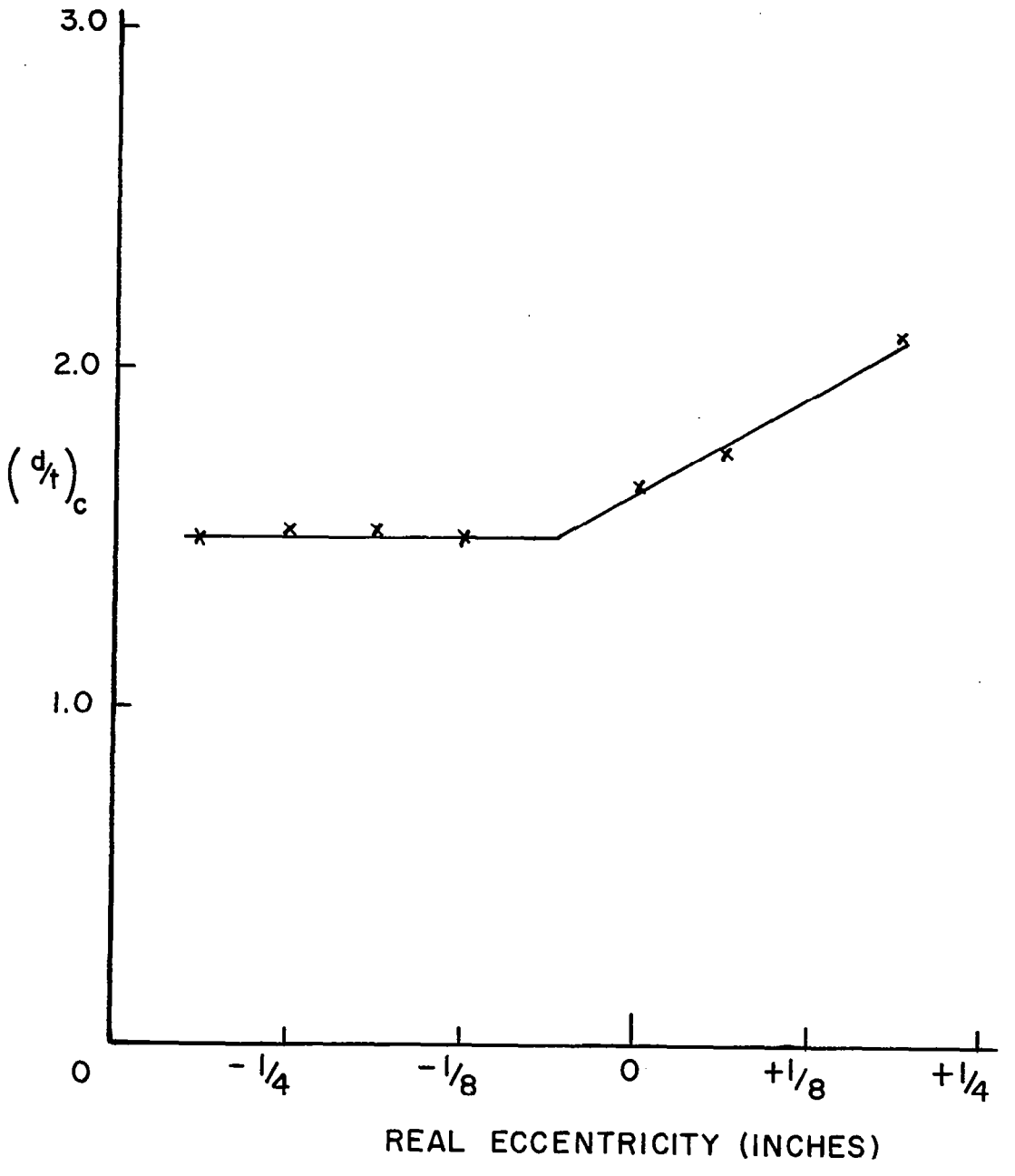

FIG. 5 CRITICAL DEFORMATION DEPTH VS. ECCENTRICITY

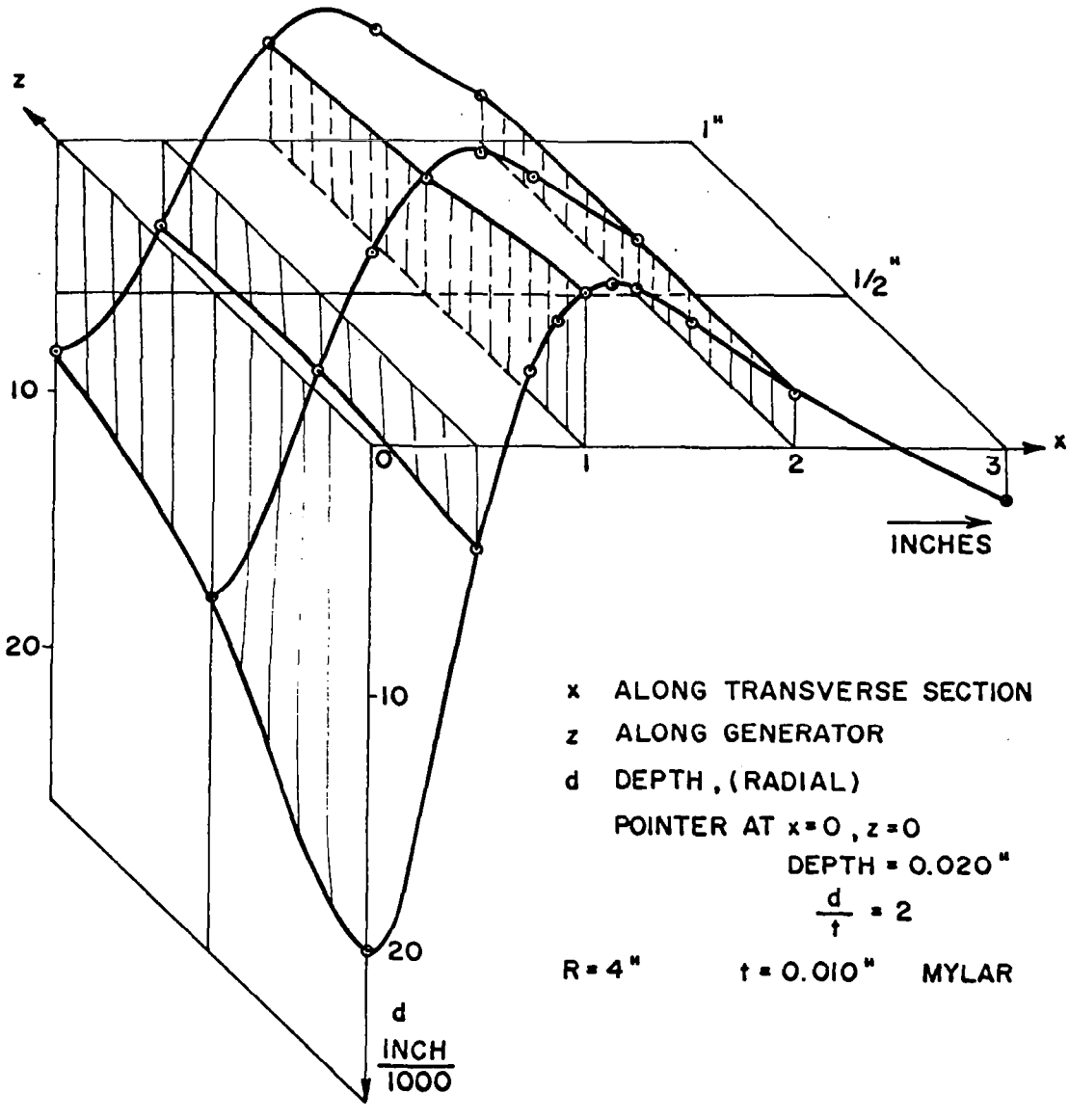

FIG. 6 TYPICAL DEFORMATION SHAPE

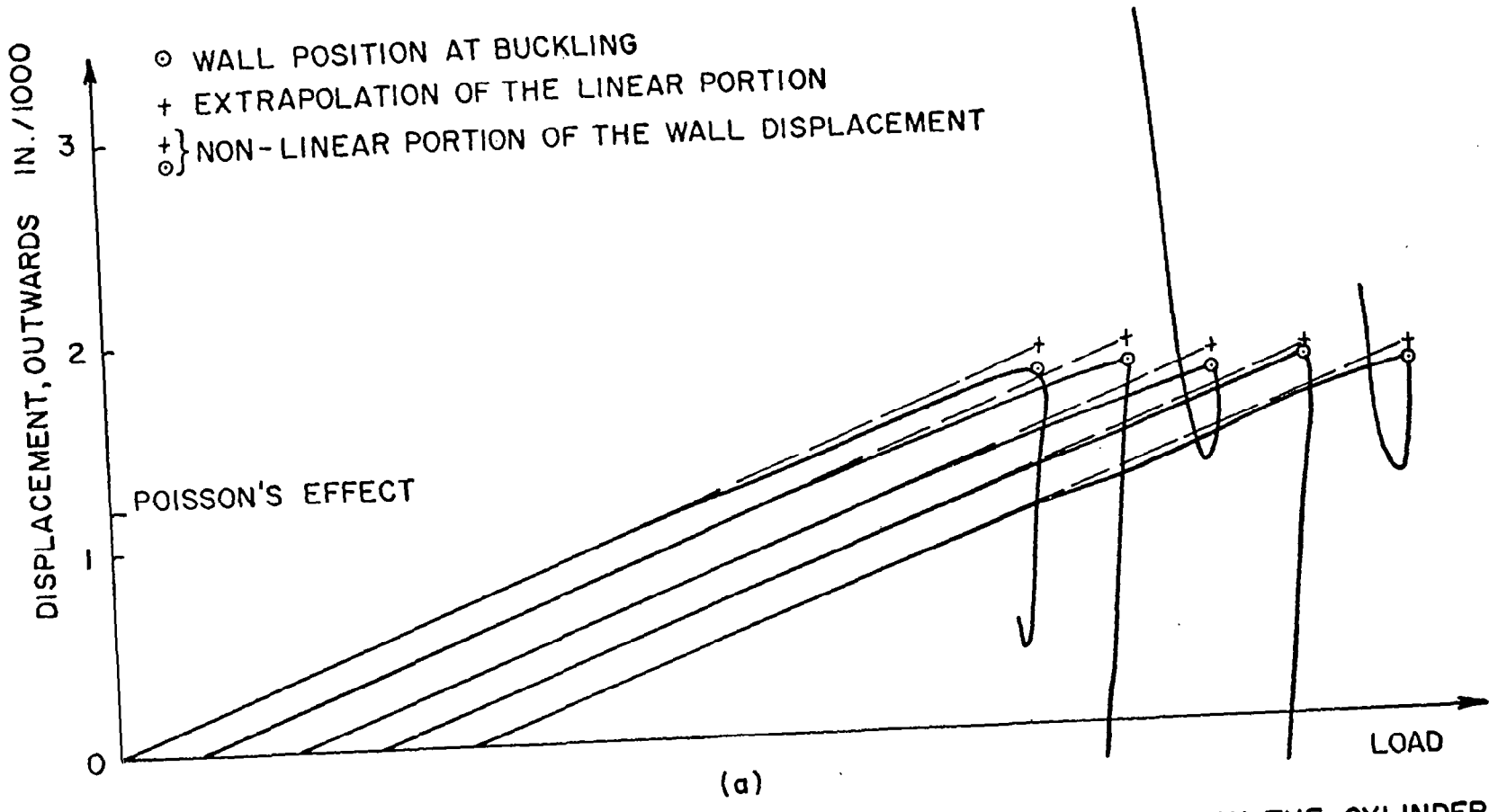

FIG. 7 LOAD DISPLACEMENT CURVES FOR TYPICAL POINTS ON THE CYLINDER

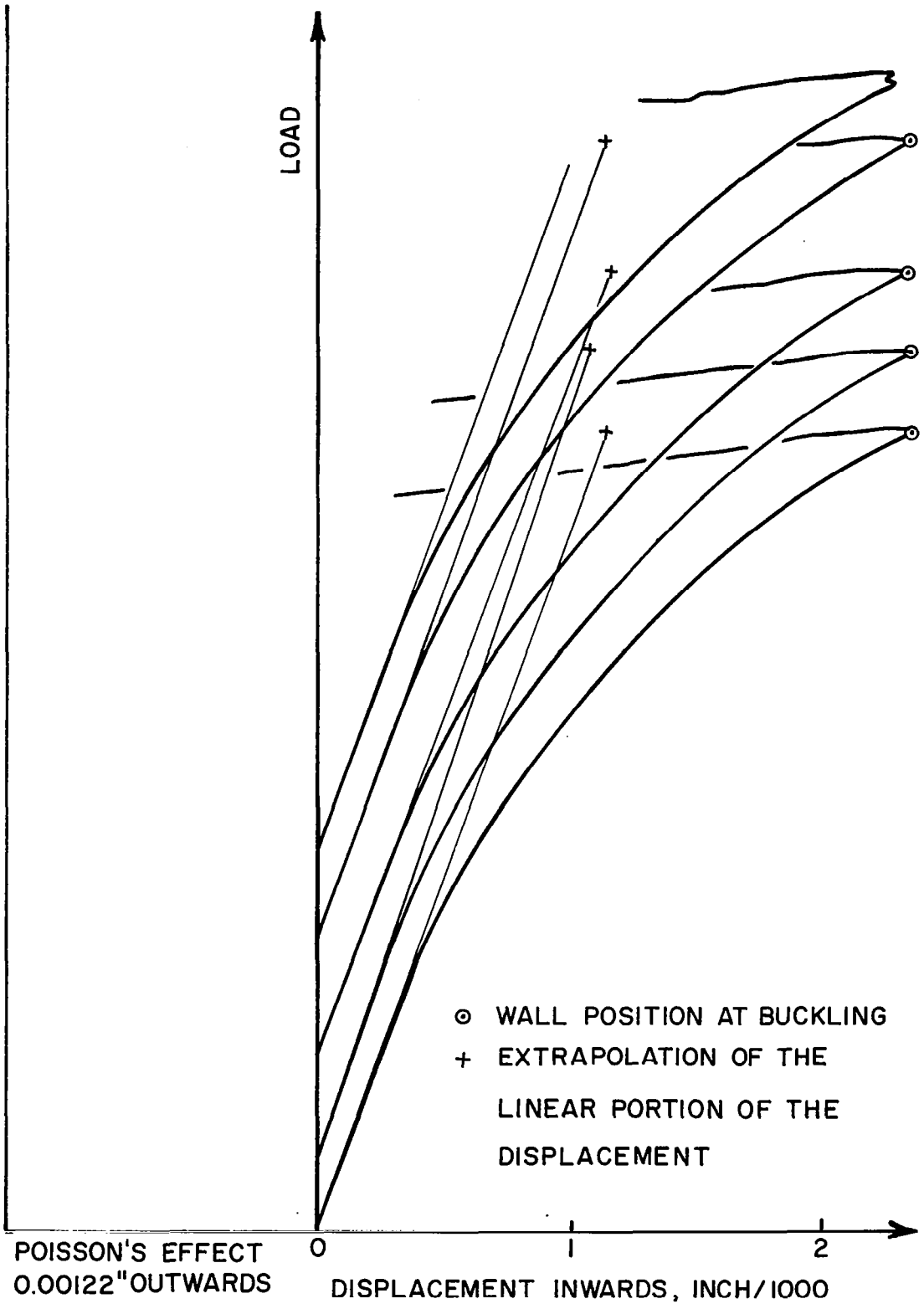
LOAD
⊙ WALL POSITION AT BUCKLING
+ EXTRAPOLATION OF THE LINEAR PORTION OF THE DISPLACEMENT
POISSON'S EFFECT
0.00122"OUTWARDS
0
1
2
DISPLACEMENT INWARDS, INCH/1000

FIG. 7b

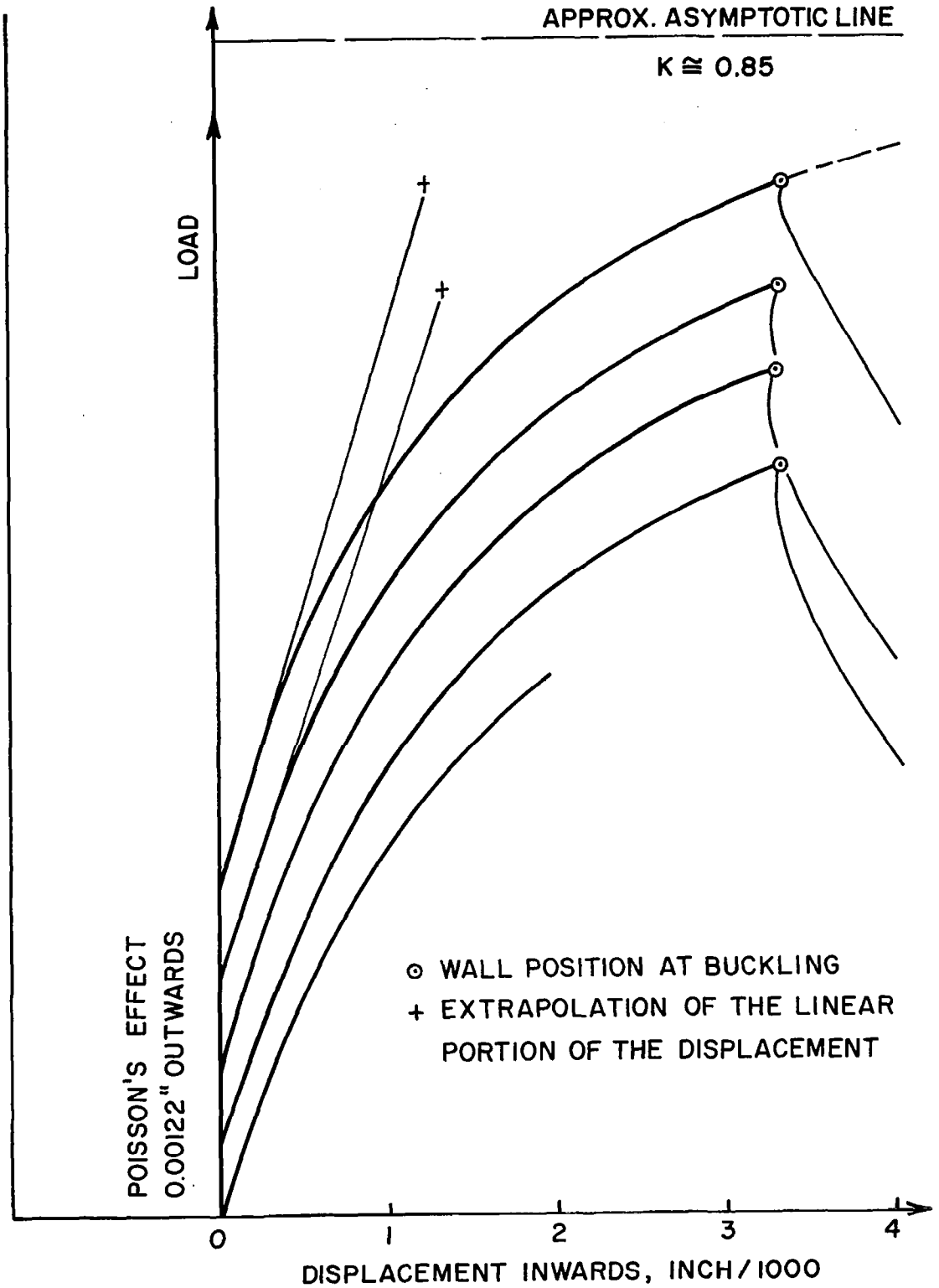
APPROX. ASYMPTOTIC LINE
K ≅ 0.85
LOAD
POISSON'S EFFECT
0.00122" OUTWARDS
⊙ WALL POSITION AT BUCKLING
+ EXTRAPOLATION OF THE LINEAR
PORTION OF THE DISPLACEMENT
0
1
2
3
4
DISPLACEMENT INWARDS, INCH/1000

FIG. 7c

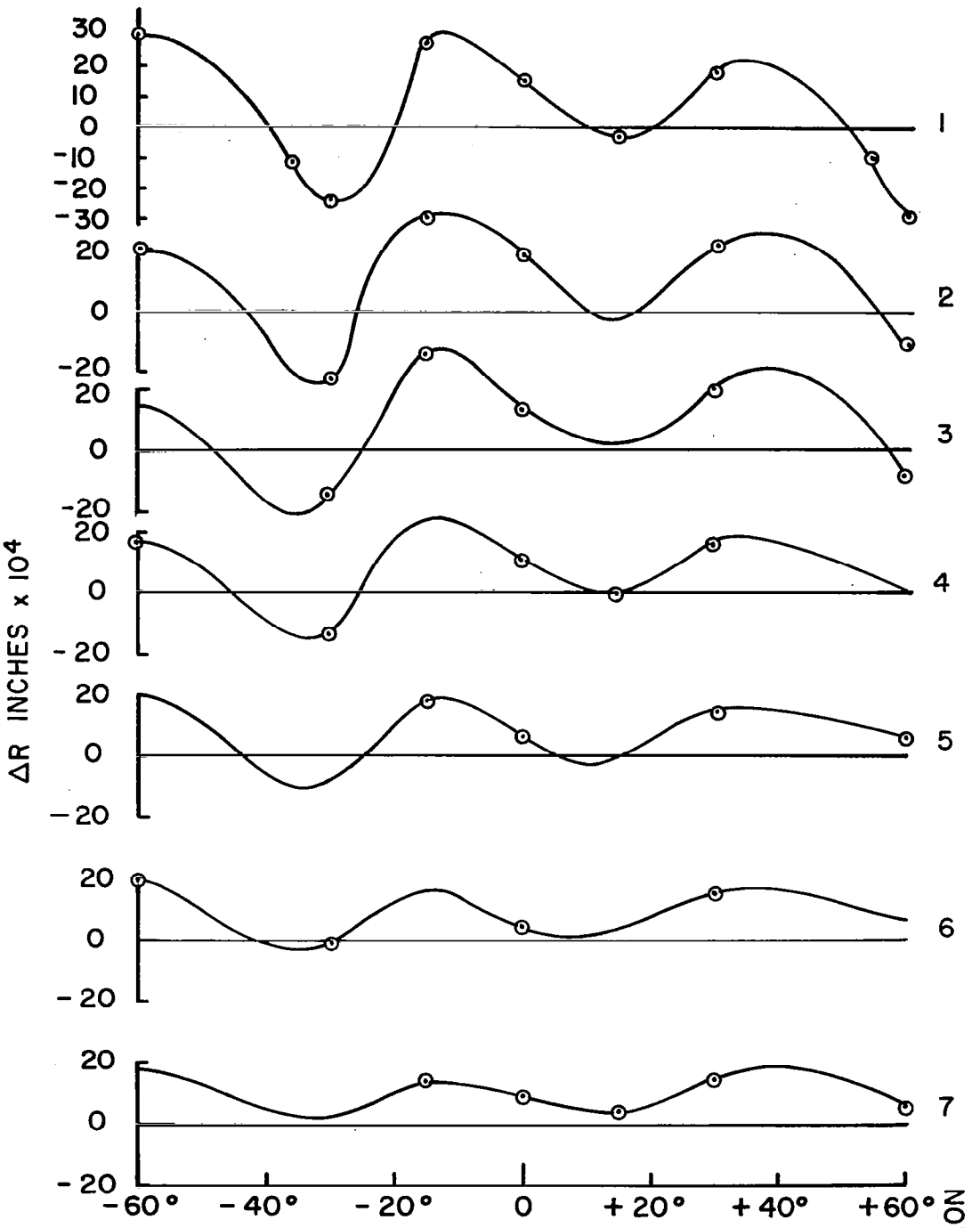

FIG. 8 RADIAL DISPLACEMENTS AT VARIOUS AXIAL DISTANCES ALONG CYLINDER AT $P_{cr.}$ (+OUTWARD)

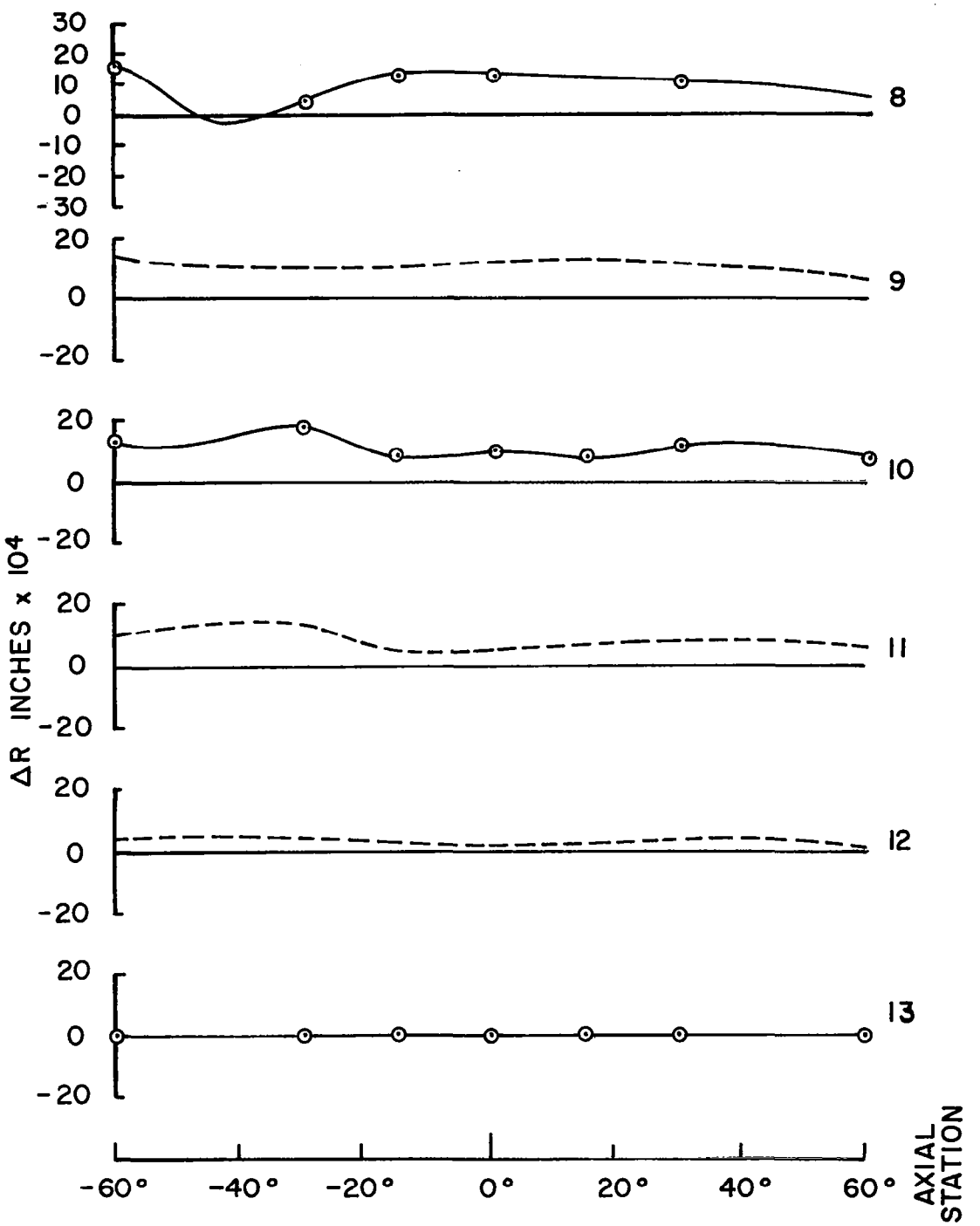
30
20
10
0
-10
-20
-30
8
20
0
-20
9
20
0
-20
10
20
0
-20
11
20
0
-20
12
20
0
-20
13
ΔR INCHES x 10⁴
-60°
-40°
-20°
0°
20°
40°
60°
AXIAL STATION

FIG. 8 (CON'T.)

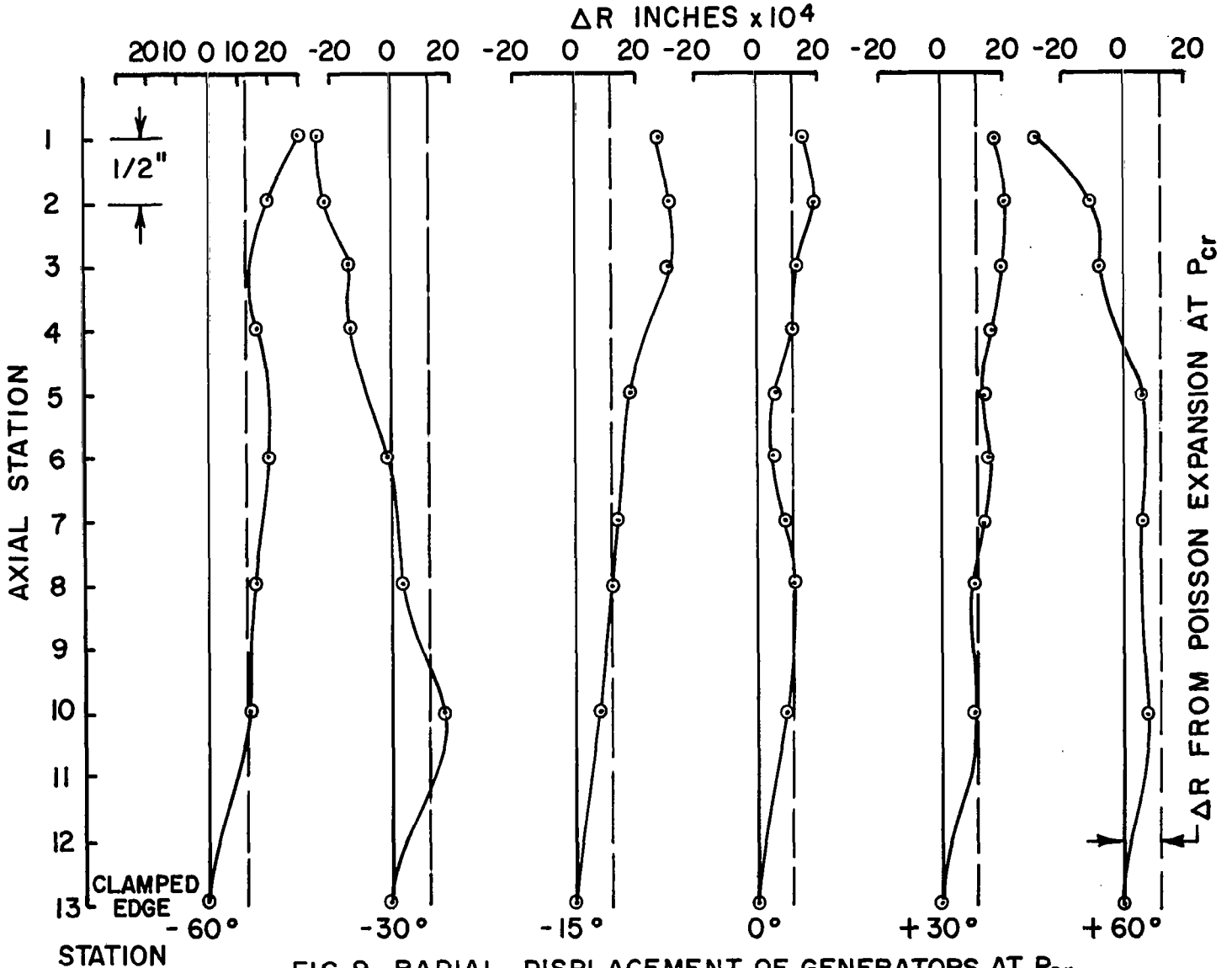

FIG. 9 RADIAL DISPLACEMENT OF GENERATORS AT P_{cr}

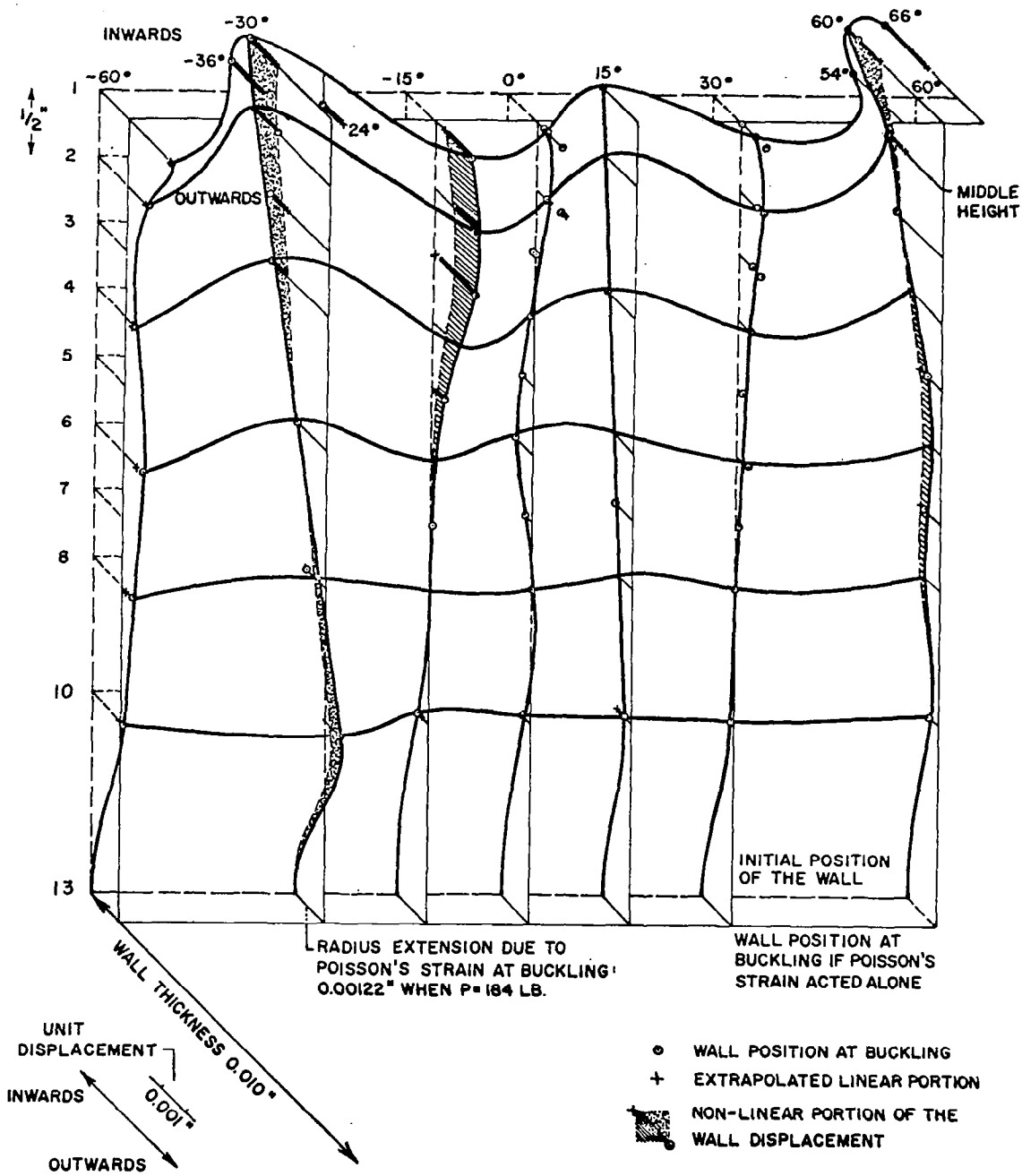

FIG. 10 CYLINDER DEFORMATION AT BUCKLING

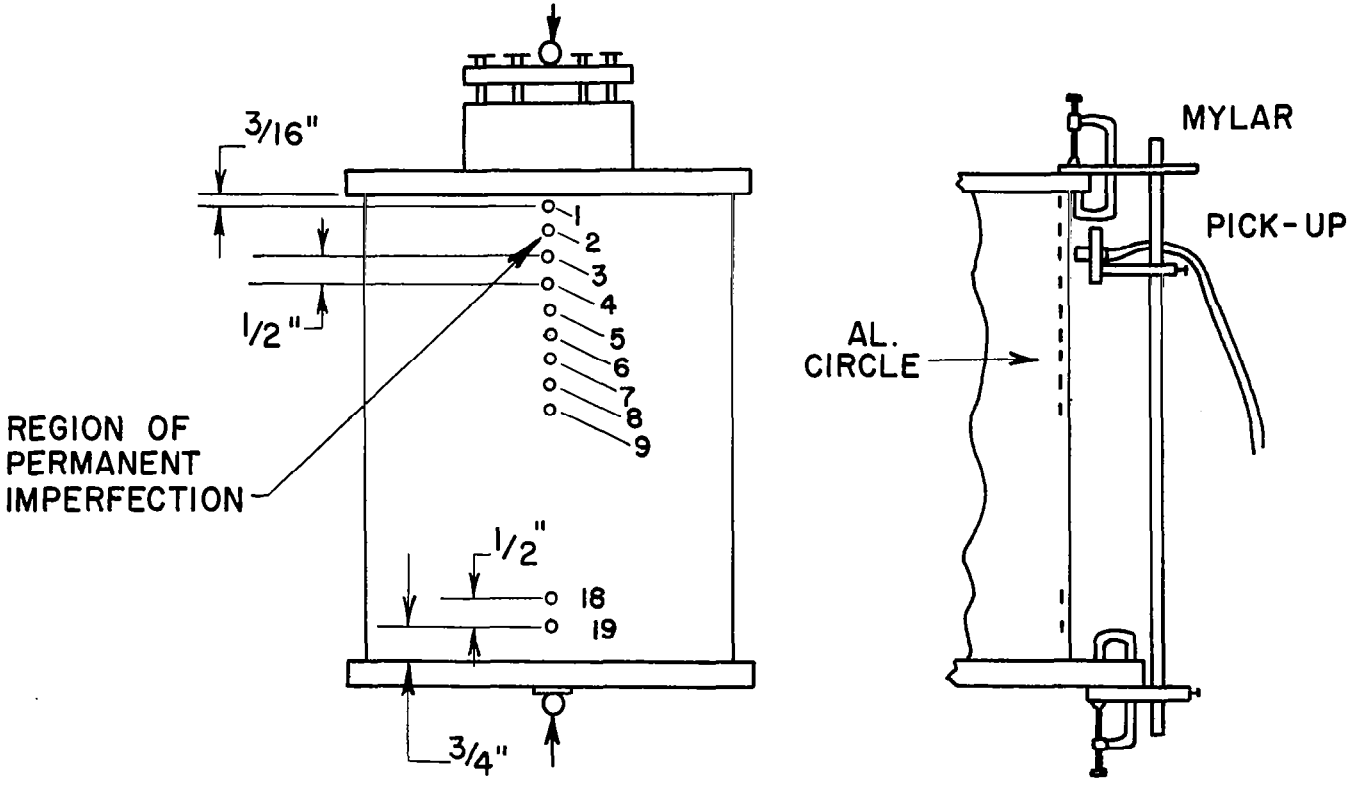

FIG.11 EXPERIMENTAL SET-UP FOR SERIES III TESTS

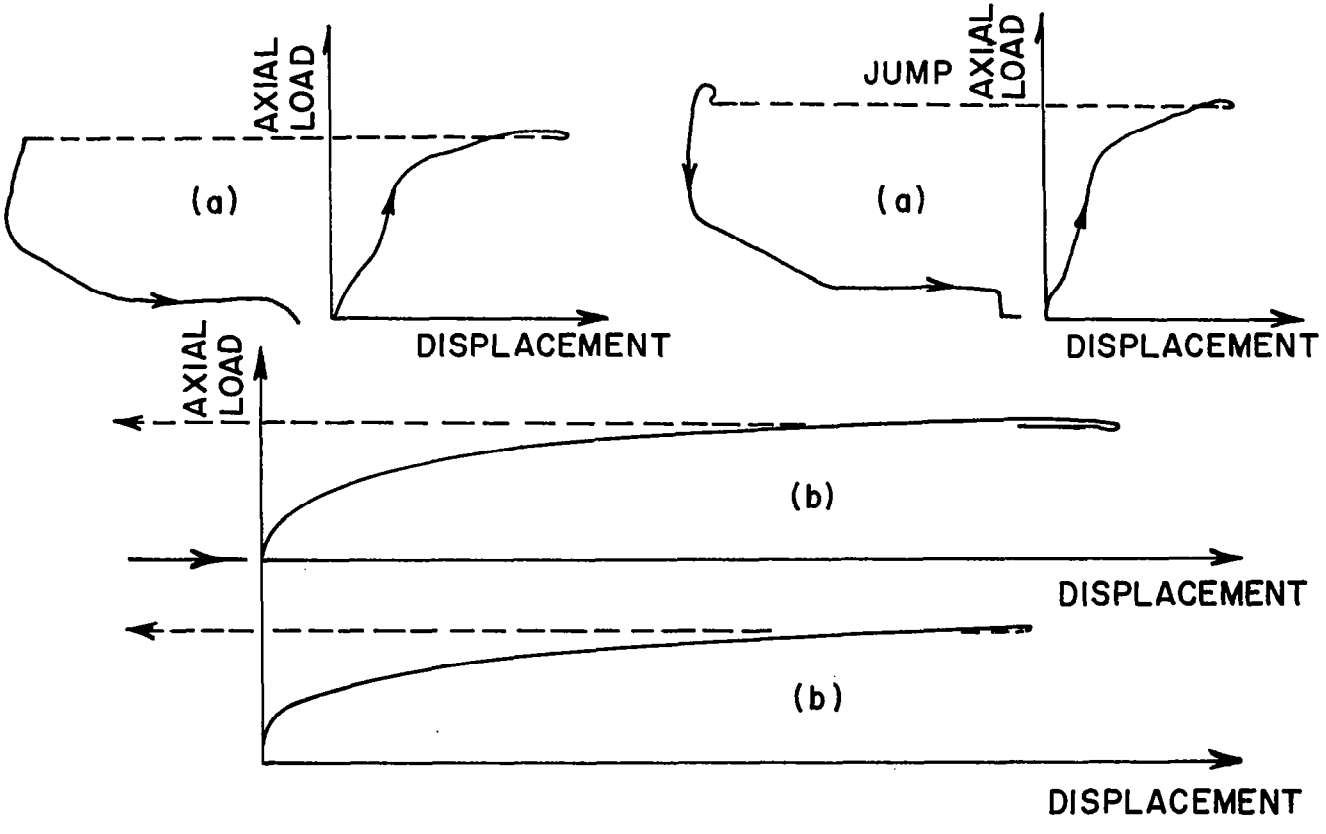

FIG. 12 LOAD DISPLACEMENT CURVES FOR POINT I AT DIFFERENT LOADS. (a) LOW AMPLIFICATION (b) HIGH AMPLIFICATION

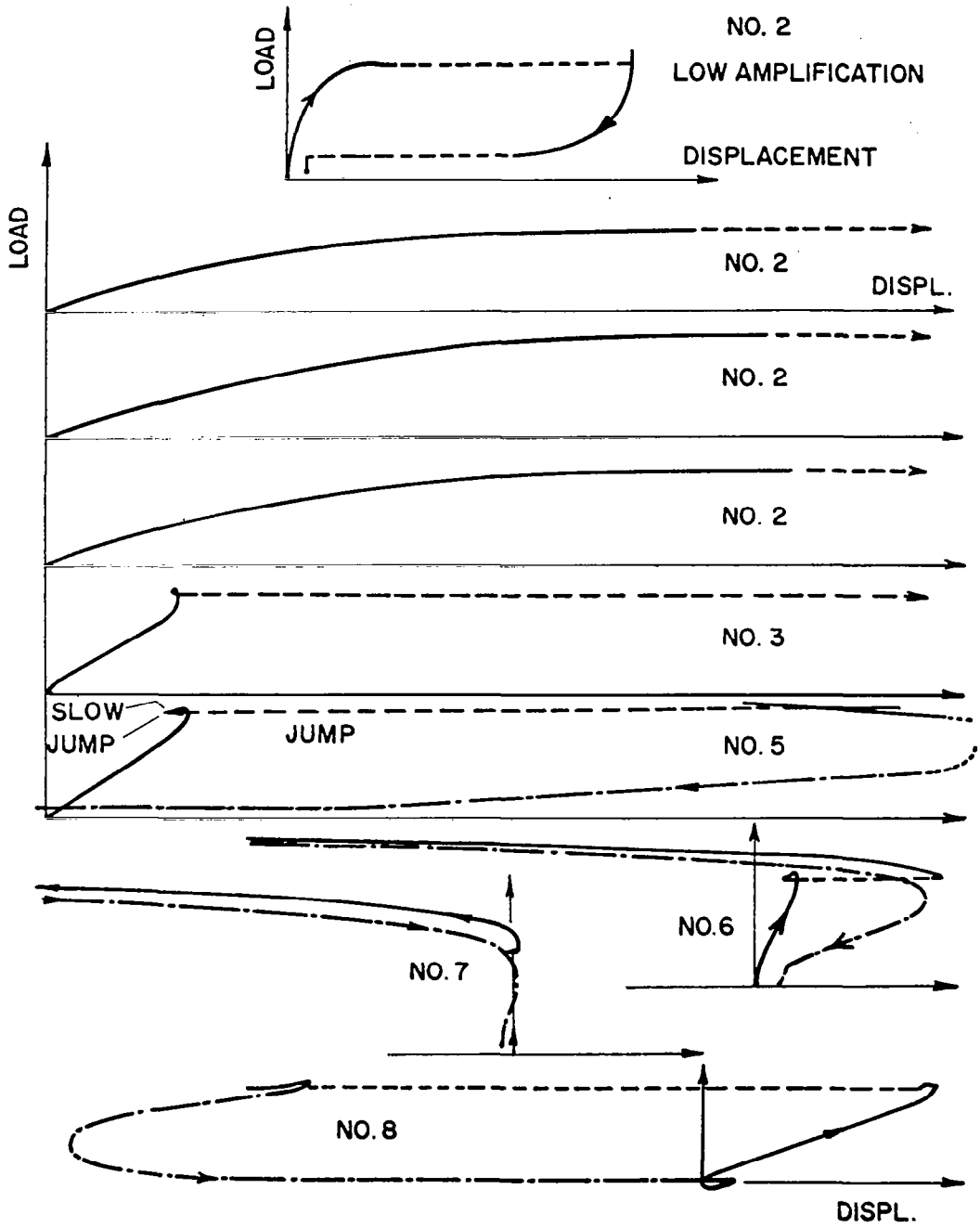

FIG. 13 TYPICAL LOAD DISPLACEMENT CURVES

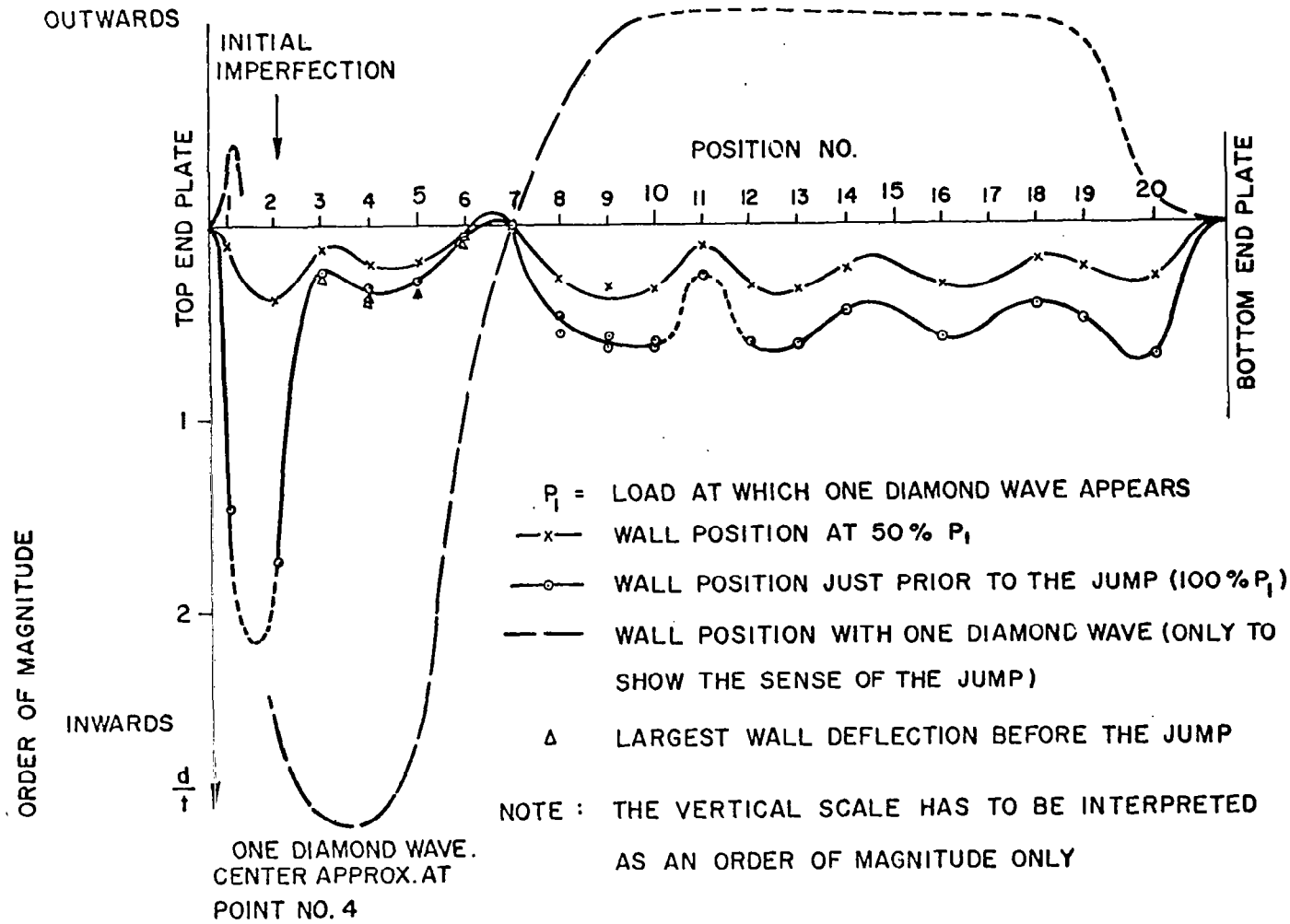

FIG. 14 DISPLACEMENT ALONG A GENERATOR CONTAINING AN INITIAL DEFORMATION AT A POINT

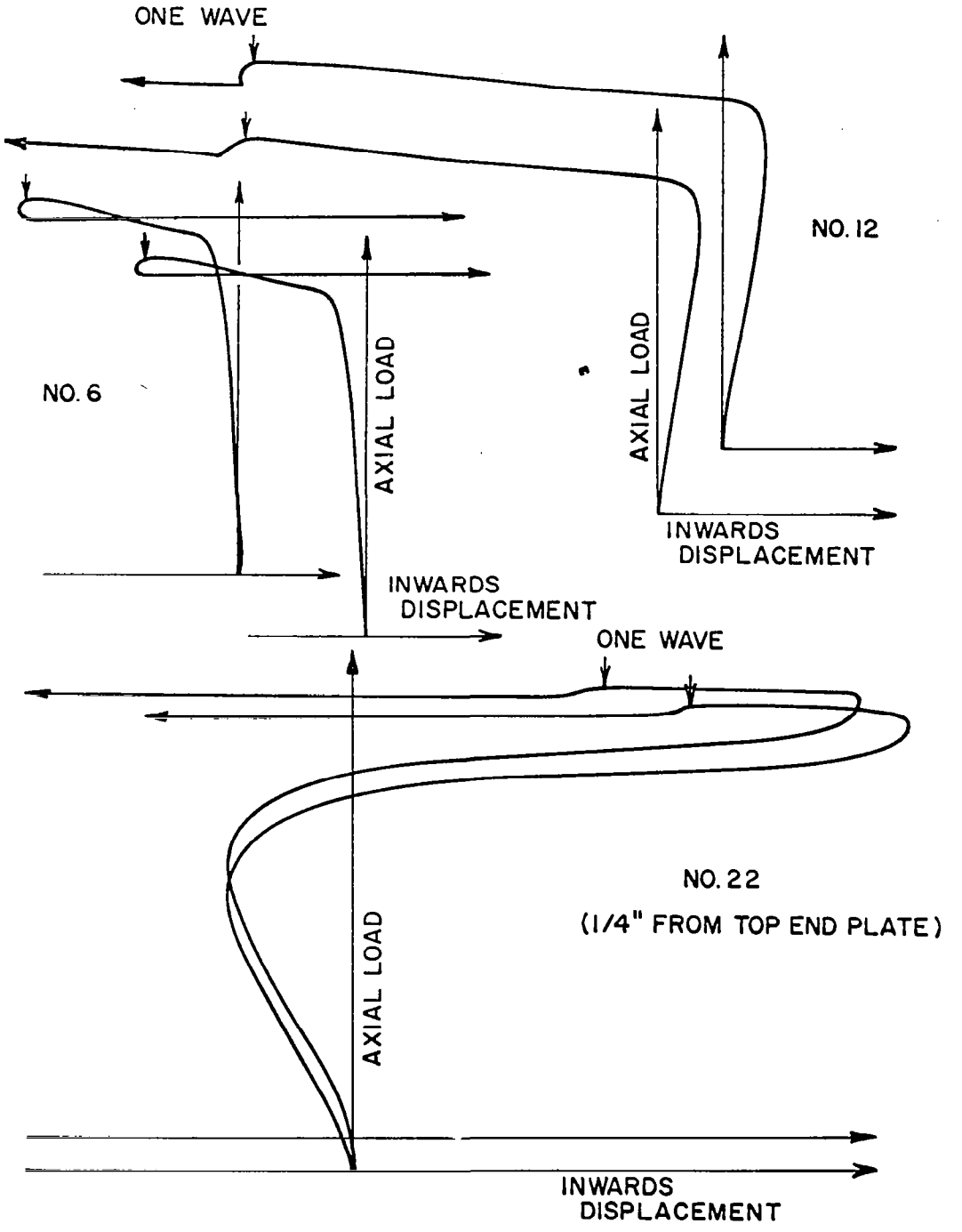

FIG. 15 DISPLACEMENT CURVES AT VARIOUS POINTS DURING LOADING